COVER PAGE

Summary of the Campus Electric System Operation with the Installed Campus CPV Resources

REPORT DRAFT 2.0
DATE: March 2014

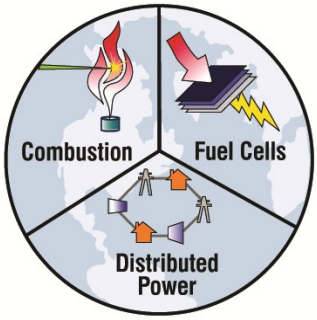

Submitted To:

Robert McConnell
Amonix Project Director
Office : 562-200-7741
Email: bob@amonix.com

Submitted By:

Professor Scott Samuelsen, Director
Professor Jack Brouwer, Associate Director
Advanced Power and Energy Program
University of California, Irvine
Tel: 949-824-7302 x11-221
Email: gss@uci.edu; jb@apep.uci.edu

March 2014

Executive Summary

Amonix, Inc., in partnership with the University of California, Irvine (UCI) and the National Renewable Energy Laboratory (NREL), is conducting a project to install up to nine Amonix 7700 systems on the UCI campus for studies of grid integration and reliability. The project purpose is to provide technology and knowledge advancements that enable California to deploy a high percentage of ultra clean, secure and reliable solar electric generation at the lowest possible cost. The Amonix 7700 is a concentrating photovoltaic (CPV) system using inexpensive Fresnel lenses to focus the equivalent of 500 suns onto small 39% efficient solar cells. A 7700 has seven MegaModules that each produce approximately 10 kW (DC) and, with dimensions of 77' by 49', is the world's largest pedestal-mounted solar power generator. As part of this deployment the Advanced Power and Energy Program (APEP) at UCI is identifying and documenting the challenges and opportunities for installing large CPV systems in UCI's distribution circuits. APEP is assessing the preferred CPV integration by determining the value of peak solar generation and benefit of solar generation coordination with combined heat and power systems and demand management. In a set of additional tasks, Amonix and NREL are jointly conducting lifetime and reliability modelling by correlating failures observed in accelerated testing of CPV components with measured weather data and with failures observed in the field deployment of the systems on the UCI campus and elsewhere.

The R&D tasks aim to address key integration barriers in installing and operating Amonix CPV systems in a distributed grid. Additional R&D tasks address the lifetime and reliability validation of Amonix systems. The UCI tasks are as follows:

(1) Subtask 2.3: Distributed CPV electrical interconnection – to establish detailed monitoring of nine Amonix 53 kW CPV systems and the associated circuits.
(2) Subtask 2.4: Preferred CPV Integration Assessment – to assess and develop the preferred integration and operation strategies for CPV systems integrated with complementary combined heat and power (CHP) and dispatchable air conditioning systems.
(3) Subtask 2.5: Coordinate with RESCO and SCE – to coordinate with the RESCO project funded by the California Energy Commission and establish a partnership with Southern California Edison.

This report summarizes the operation of the campus distribution system with regard to the installed campus CPV resources (Subtask 2.3). This involves impacts on circuit operation. The report begins with discussing the data collection installed to monitor the impacts of the Amonix CPV systems on the campus circuits as well as assess the performance of the CPV systems. The report discusses the development of models for the campus electric system to evaluate the impacts of increased CPV installations on campus circuit operation. An experimental platform was also developed to further investigate impacts of CPV installations on circuits.

Two Amonix CPV 7700 system were installed at the eastern side of the University of California, Irvine campus at 33° 38' 23.29" N, 117° 49' 30.33" W. Both systems were connected to the UC-9 12kV feeder. Each system contains a 21 x 12 module CPV array mounted on a two-axis tracker and an 82kW Solectria 7700 PVI inverter. The systems have a combined peak output rating of approximately 120kW. The CPV system performance was assessed using the data collected from

the CPV systems. The CPV system operated with an overall efficiency of 23.63% and a cut in threshold of 350 W/m^2. No correlation between ambient temperature and system efficiency were found. Data collected also revealed that the combined solar generation from the CPV systems and the fixed PV systems coincides with demand during winter months and precedes demand by approximately 1 hour during summer months and serves approximately 4% of peak campus load. Initial analyses done by scaling up the temporal current combined solar generation showed that the maximum allowable combined solar generation (without curtailment or energy storage capabilities) while meeting minimum utility import requirements is approximately 3 MW. Data also revealed excessively high terminal voltages. Possible remedies include increasing the CPV-7700 to ARC-MCC conductor size, operating at a lagging power factor, or utilizing a dedicated step-up transformer to directly couple to the 12kV feeder.

Circuit simulations were performed using two modeling platforms: ETAP and MATLAB. ETAP was used for campus wide traditional load flow studies while MATLAB was used for detailed sub-circuit and investigational simulations. These circuit simulations provided several important conclusions regarding campus circuit operation with installed CPV systems:

- Voltage fluctuations due to changes in power production attributed to cloud cover and coastal fog are adequately buffered by utility voltage up to an installed CPV capacity of 14 MW.
- Net reverse power flow at the ARC-MCC is achieved at approximately 380 kW installed CPV capacity.
- To achieve the highest efficiency, it is recommended that CPV installations occur until the CPV capacity equals the peak electrical demand at that circuit location. Further CPV installations result in increased line losses.
- UC-3, 4, and 10 are ideal candidates for large installations at the 480V level due to their proximity to the UCI substation.
- Installation near the UCI substation results in the greatest voltage stability and minimizes line losses.
- UC-1, 2, 5, 6, 8, and 9 are unable to support any CPV above approximately 360kW at any individual location at the 480V level without exceeding ANSI voltage tolerance limits while operating at unity power factor. Installation at the 12kV feeder may alleviate this issue.

1 Introduction

The goal of this project is to provide technology and knowledge advancements to enable California to deploy a large amount of ultra clean, regionally secure solar electric generation at the lowest possible cost. To meet this goal, four tasks were addressed. Each proposed task is complementary and specifically developed to address the most critical challenges and opportunities to increase solar deployment in California. In particular, UC Irvine was responsible for two tasks:

- Subtask 2.3 – Distributed CPV Electrical Interconnection
- Subtask 2.4 – Preferred Integration Assessment

The objectives of UC Irvine's tasks are described below:

Subtask 2.3 – Distributed CPV Electrical Interconnection:
The objective of this task is to establish detailed monitoring of nine Amonix 53 kW HCPV systems and associated circuits at the University of California, Irvine. In the process of deploying the units, many of the challenges and opportunities to install large HCPV installations on distribution circuits will be identified and documented. Specifically, information regarding the impact of large HCPV installations on distribution electric infrastructure are to be identified. Lessons learned will provide valuable data and experience to rapidly evaluate future site deployments.

Subtask 2.4 – Preferred Integration Assessment:
The objective of this task is to evaluate the value of peak solar generation and benefit of solar generation coordination with combined heat and power systems and demand management. By coordinating with other gas turbine generators and dispatchable loads (e.g., air conditioning with thermal energy storage, and future electric vehicles), further reduction in the end users' utility bills per unit of solar installed capacity can be seen. In this way, the cost of solar energy is decreased not by reducing the direct cost of solar energy, but by the development of better grid integration and energy management strategies.

This report is the second deliverable due under Subtask 2.3 and summarizes the operation of the campus electric system with regard to the installed campus CPV resources. The first report section discusses 1) the Amonix installation on the UC-9 circuit, 2) data collection, and 3) assesses CPV system performance. The second report section discusses the development of electric and CPV system models and how those models were used to evaluate the impacts of CPV systems on the UCI distribution system.

2 Electrical Interconnection, Data Collection, and Performance of the Amonix System

2.1 Amonix CPV -7700 System

The Amonix CPV 7700 system is a dual axis tracking concentrated photovoltaic system capable of producing approximately 60kW of grid-tied power. Two CPV 7700 system have been installed at the eastern side of the University of California, Irvine campus at 33° 38' 23.29" N, 117° 49' 30.33" W. Each system contains a 21 x 12 module CPV array mounted on a two-axis tracker and an 82kW Solectria 7700 PVI inverter. The systems have a combined peak output rating of approximately 120kW, and the maximum observed AC power output was measured at 126.19kW at 999.94W/m^2 direct normal irradiance (534m^2 lens area). The average system efficiency has been measured at 23.63%.

Figure 1. Dual Amonix CPV-7700 Systems at the University of California, Irvine.

2.1.1 Instrumentation

Individual module currents are measured with current sensors from Obvius Energy. The inverter AC output of Unit A is metered with an Electro Industries Shark 100 power meter/tranducer and Unit B is similarly measured with an Elkor WattsOn power meter. An additional Electro Industries Shark 200 power meter/transducer meters the combined system output. All power meters/tranducers measure real power, reactive power, voltages, frequency and energy production. The Shark 200 meter also measures harmonic distortion. The two Solectria 7700 inverters also measure operating conditions (system temperature, power output, voltage and current inputs). An on-site meteorological station has been installed to support data collection at the UCI site. Instrumentation includes a pyrometer, anemometer, and thermometer. Data have been collected and archived beginning June 5th, 2012 at a 1-minute granularity from each instrumentation device. The following figure shows system instrumentation components and the data recorded from each device.

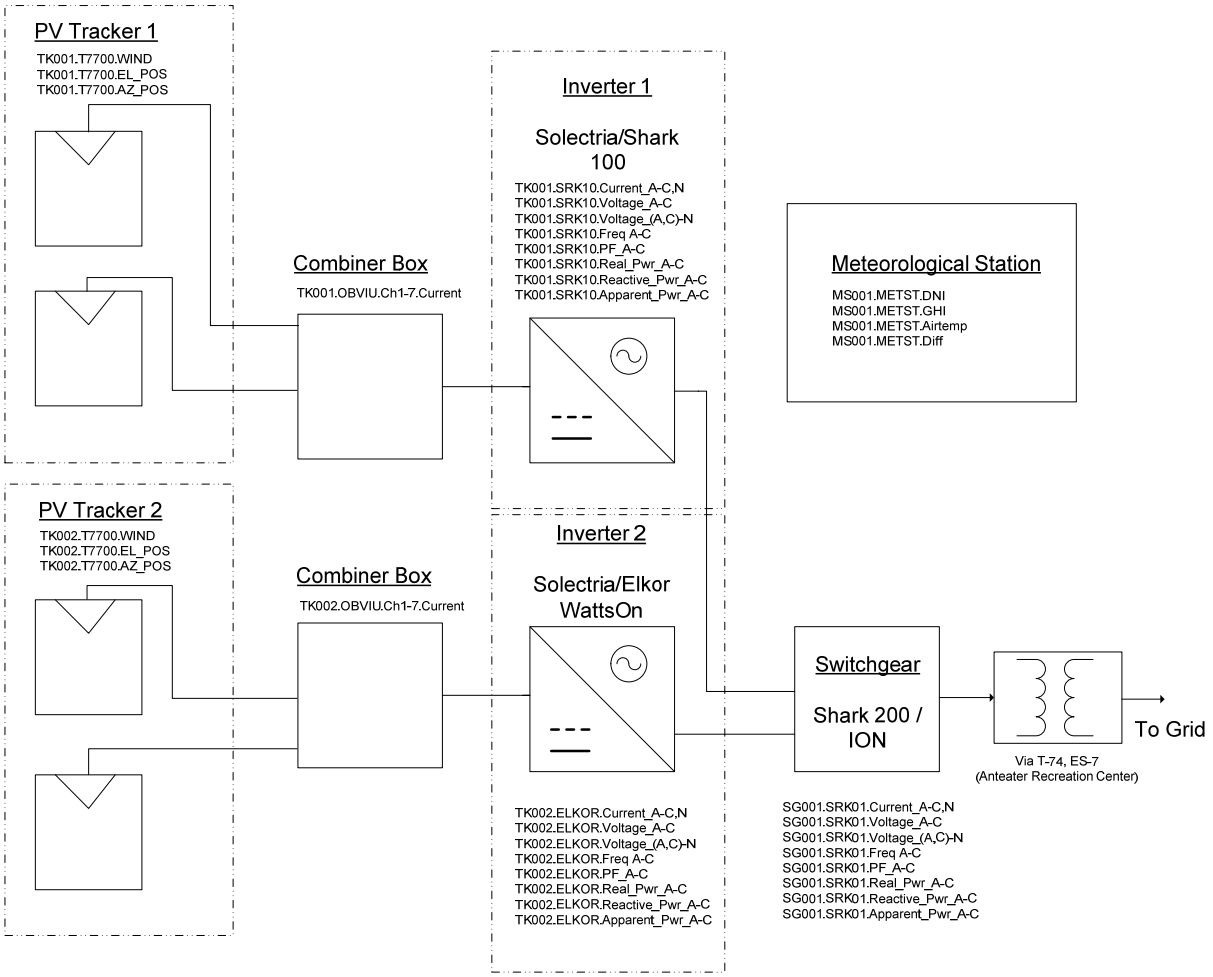

Figure 2. Metering Equipment.

2.2 Amonix Electrical Interconnection

The UCI microgrid circuit consists of 10 12.47kV subcircuits (UC 1-10) that originate from a 56MVA, 66 - 12.47kV dual fed substation connected to the Southern California Edison transmission circuit. The Amonix site is connected to the UCI distribution circuit via a 2MW 12.47kV - 480V transformer on the UC-9 branch circuit. This transformer also services the student recreation center (ARC) which averages a load of approximately 300kW. The remainder of the loads installed on the UC-9 circuit total average approximately 4MW and are serviced by a total of 31 MW of nameplate transformer capacity. Two 2.7 MVAR capacitor banks provide reactive power support at the main substation.

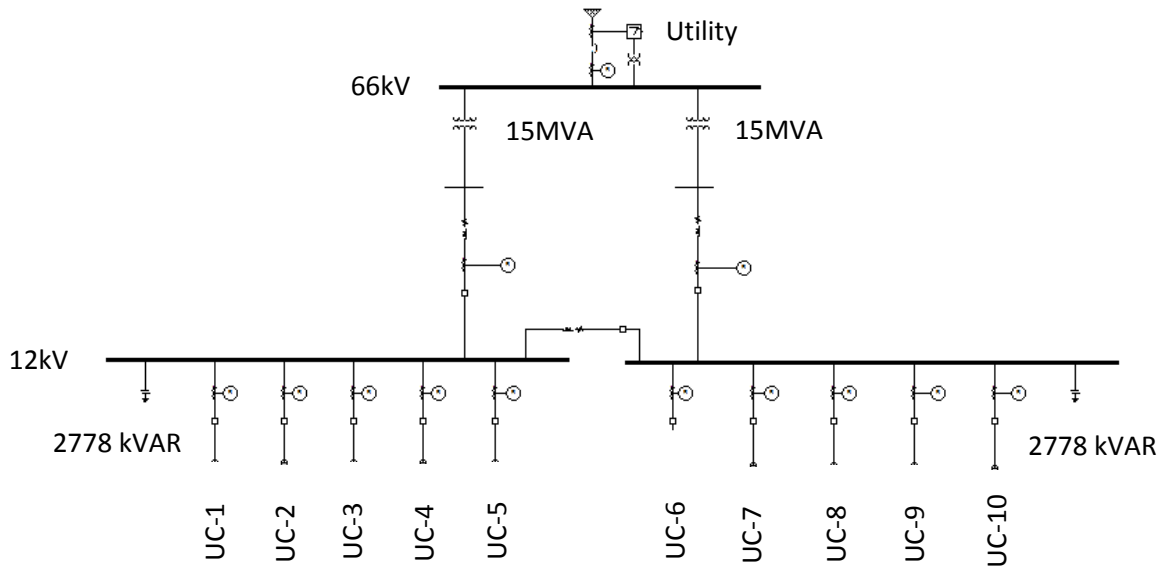

Figure 3. UCI Utility Connection and Main Switchgear

Table 1. UC1-9 Subcircuit Details.

Circuit	UC-1	UC-2	UC-3	UC-4	UC-5	UC-6	UC-7	UC-8	UC-9	UC-10
Peak Load (MW)	0.446	7.4	5.1	6.8	5.4	5.2	9.2	0.1	4.1	N/A
Existing PV (kW)	155	55	118	0	0	149	0	93	198	118
No. XMFR's.	23	9	10	5	7	40	N/A	3	40	2

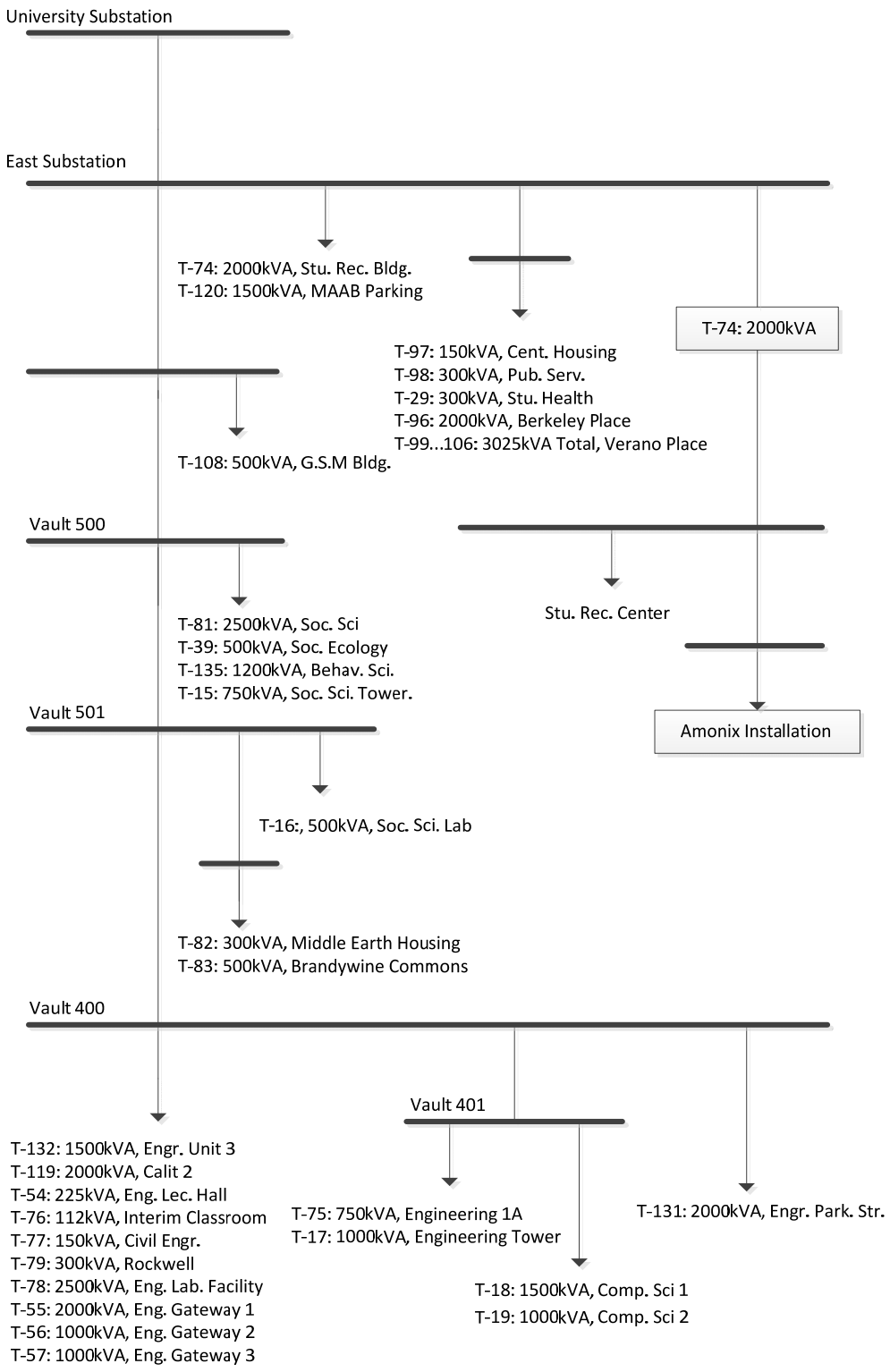

Figure 4. UC-9 Circuit Detail.

2.3 Additional Campus Generation Assets

In addition to the 120kW Amonix installation, the campus hosts an additional 900kW of flat plate PV generation located at 11 locations throughout the campus. Located downstream of the main substation, local generation assets include a 15 MW Solar Turbines Titan 130 gas turbine generator, a 5MW steam plant, and approximately 900kW of solar generation distributed through the UCI campus. During 2012, the average campus demand was approximately 21.5MW, 19MW of which was provided by local generation assets. The remaining 2.5MW of demand was provided from Southern California Edison.

The campus's unique combination of high penetration flat plate and CPV systems along with on-campus generation allows for detailed studies of PV connected to microgrid circuits. Figure 5 and Table 2 summarize additional campus solar resources.

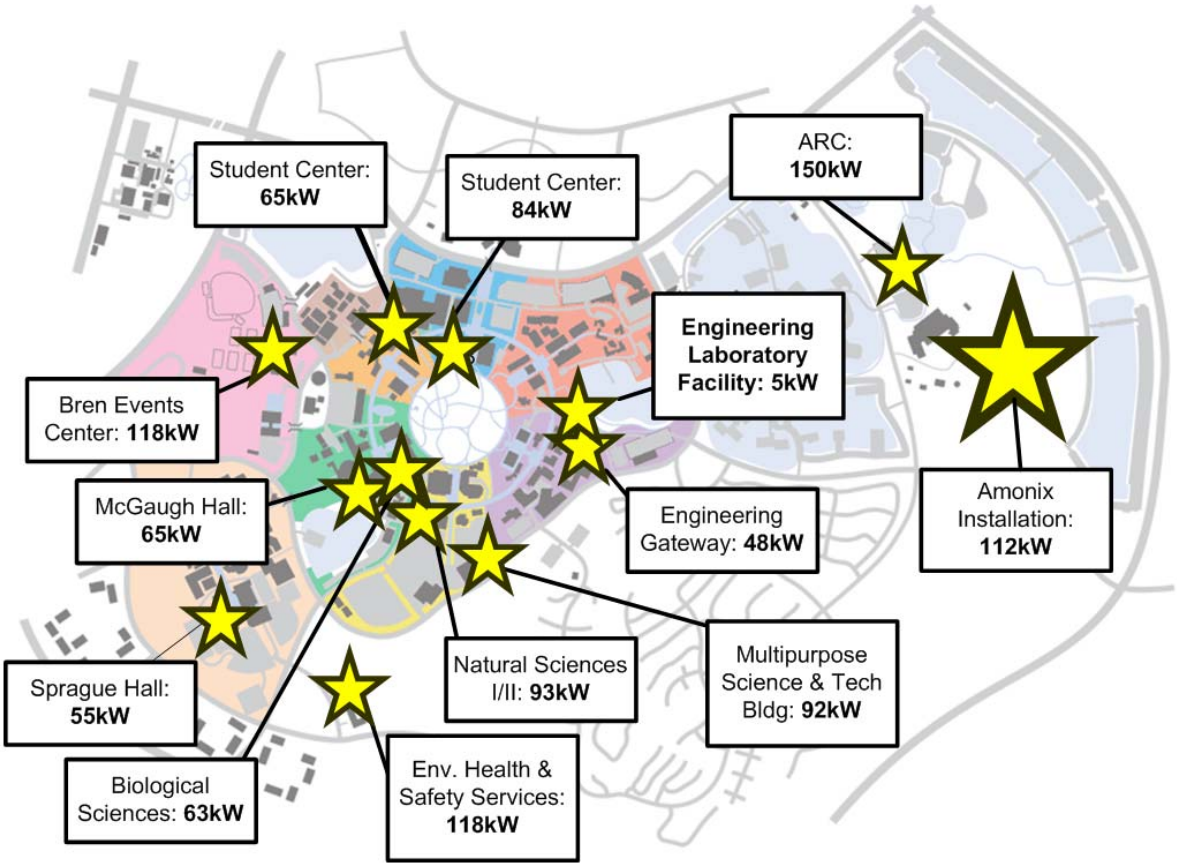

Figure 5.UCI PV Resources.

Table 2. Additional UCI PV Resources.

Location	PV Capacity (kW)	Circuit
Engineering Gateway	48	UC-9
Sprague Hall	55	UC-2 / UC-6
Biological Sciences	63	UC-1 / UC-6

McGaugh Hall	65	UC-8
Student Center 1	65	UC-6
Student Center 2	84	UC-6
Multipurpose Sci. & Tech.	92	UC-1
Natural Sciences	93	UC-8
Env. Health & Safety Sciences	118	UC-10
Bren Events Center	118	UC-3
ARC	150	UC-9

2.4 Campus Data Collection and Display

To further the understanding of the impact of the Amonix system on the entire UCI distribution circuit and predict the effect of future CPV installations / expansion, real-time campus wide metering capabilities were installed to complement data collected from the Amonix instrumentation devices. The collection of data increases the visibility of the real-time operation of the entire campus energy system, and allows for accurate simulation and optimization studies.

2.4.1 Amonix

The two Amonix systems are equipped with independent high resolution power meters that collect voltage, current, real and reactive power, frequency, phase, and harmonic distortion measurements at a 1 minute sampling rate. Current meters monitor the outputs of individual solar panel strings. Additionally an on-site meteorological weather station provides wind speed, temperature, and irradiance measurements. The data are collected by Amonix and then mirrored onto a FTP server for access by APEP researchers.

2.4.2 MelRok

To supplement data collection from the Amonix system, a campus wide monitoring solution provided by MelRok is currently being installed at UCI. The system consists of 100 building level Melrok power meters, 50 hot water temperature meters, and 32 existing 12kV ION/PowerLogic/Siemens power meters placed at strategic locations throughout the UCI microgrid. Meter placement was selected to maximize visibility of the entire UCI microgrid. A comprehensive visibility study was conducted, taking into account total and relative building load, peak demand, and other various factors. The meters measure voltage, current, real and reactive power. The data are archived into the EnergiView web-based application for storage, retrieval, and analysis. A secondary data feed directs measurement data into an APEP server via the BACNET protocol at a rate of 1 sample per second to be directly interfaced into the ETAP for real-time load flow simulations and campus energy monitoring.

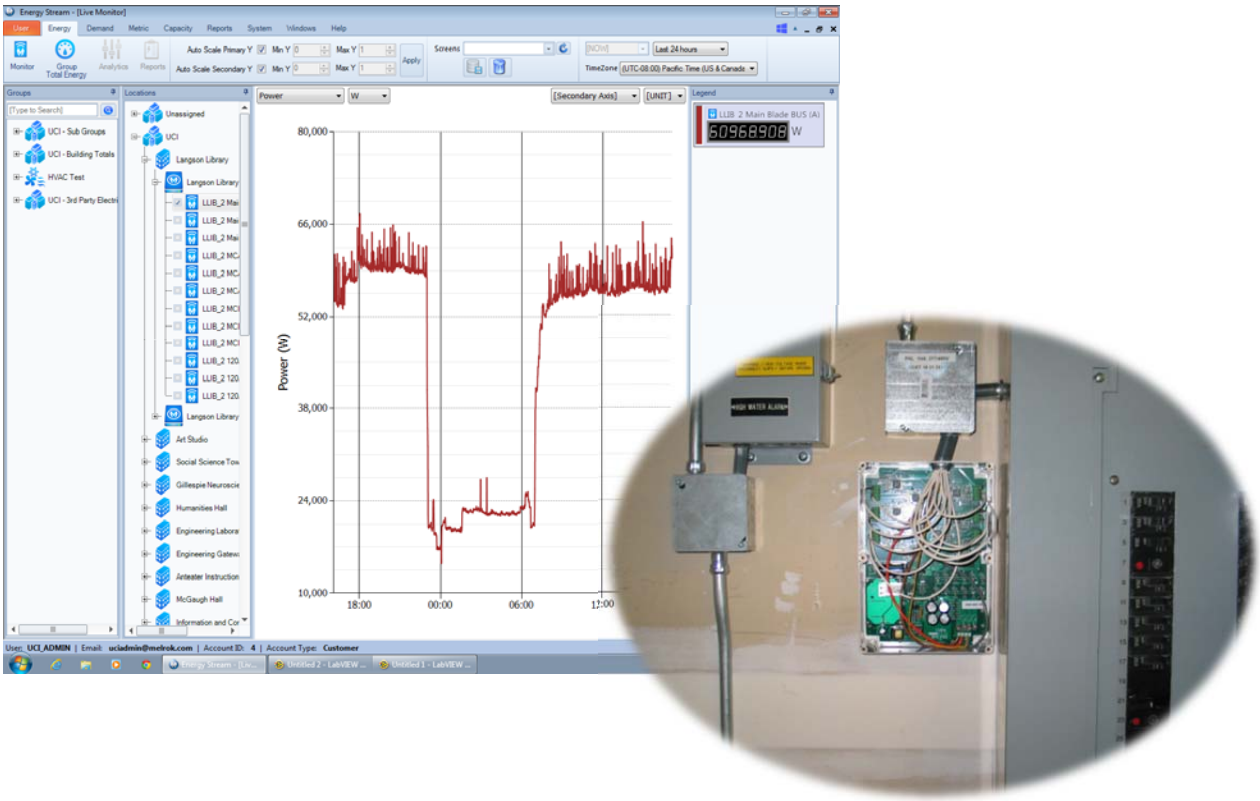

Figure 6. EnergiStream Interface and Melrok Metering Device.

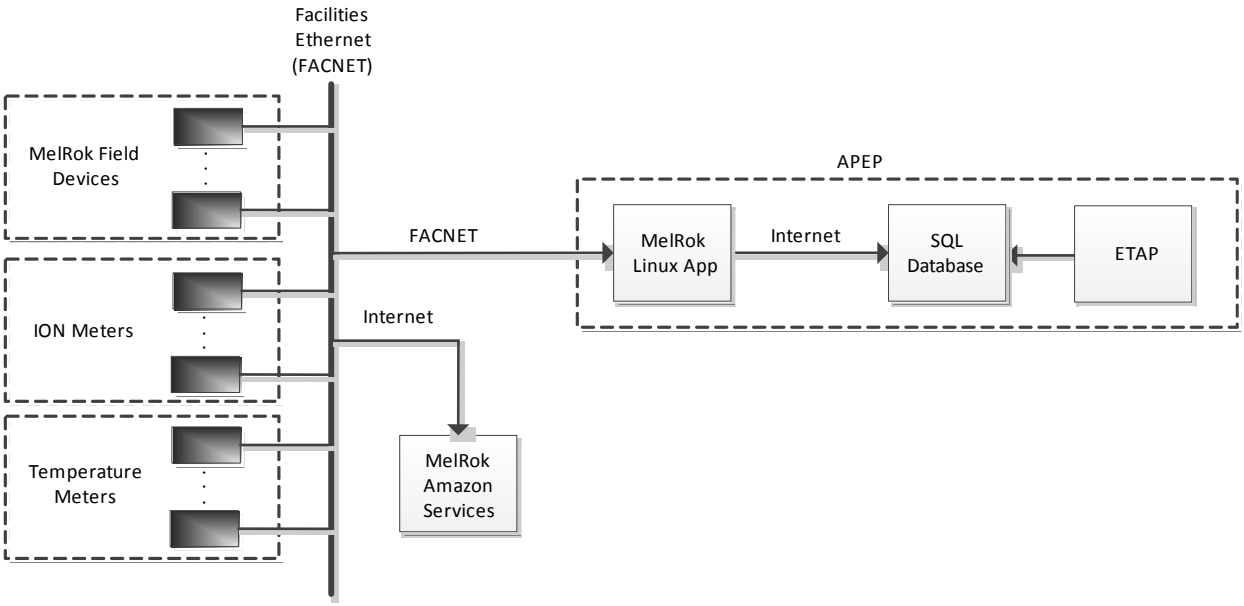

Figure 7. Melrok Data Infrastructure.

2.4.3 ETAP Real-Time

In addition to data analysis, load flow simulations were conducted in ETAP and Simulink to analyze existing and potential future UCI microgrid / CPV operation scenarios. ETAP is a commercial suite of electrical software applications capable of intelligent power monitoring, energy management, system optimization, and real-time prediction. The ETAP Real-Time software module was employed to provide online real-time load flow analysis capabilities. Available data sources from power meters, transformers, and generation equipment were combined into a unified data stream which was then utilized as ETAP simulation inputs and used to evaluate real-time microgrid operation. The UCI microgrid has over 140 building loads, 32 of which currently have online meters. Full coverage of the UCI microgrid is expected to complete by the first quarter of 2014. In the interim, loads for buildings for which data were unavailable were approximated using building square footage and type. Voltage profiles were calculated using the ETAP state load estimator and the resulting output data is transferred to a SQL server where a post-processing script converts the data to a usable form. Figure 8 is a screenshot of a load flow simulation of the Engineering Gateway building. Simulations allow for determination of overall system efficiency and determination of the maximum amount of CPV that can be installed on each respective circuit while staying in voltage bounds while taking into account intermittencies. In the future it is expected that the ETAP UCI microgrid model will assist Facilities Management in operation of the UCI microgrid through interfaces such as those shown in Figure 9.

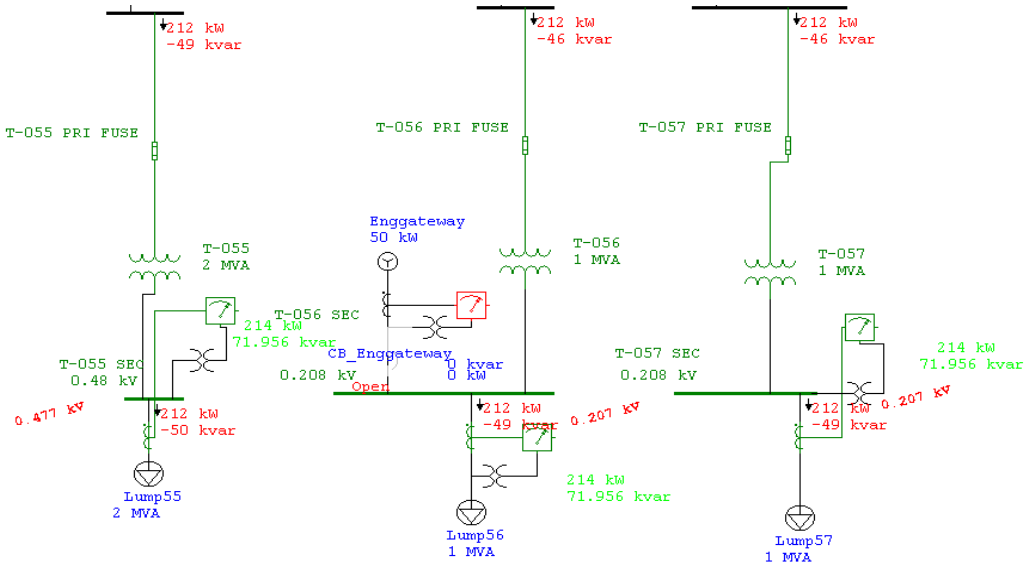

Figure 8. ETAP One-line / Load Flow Screen (Building: Engineering Gateway).

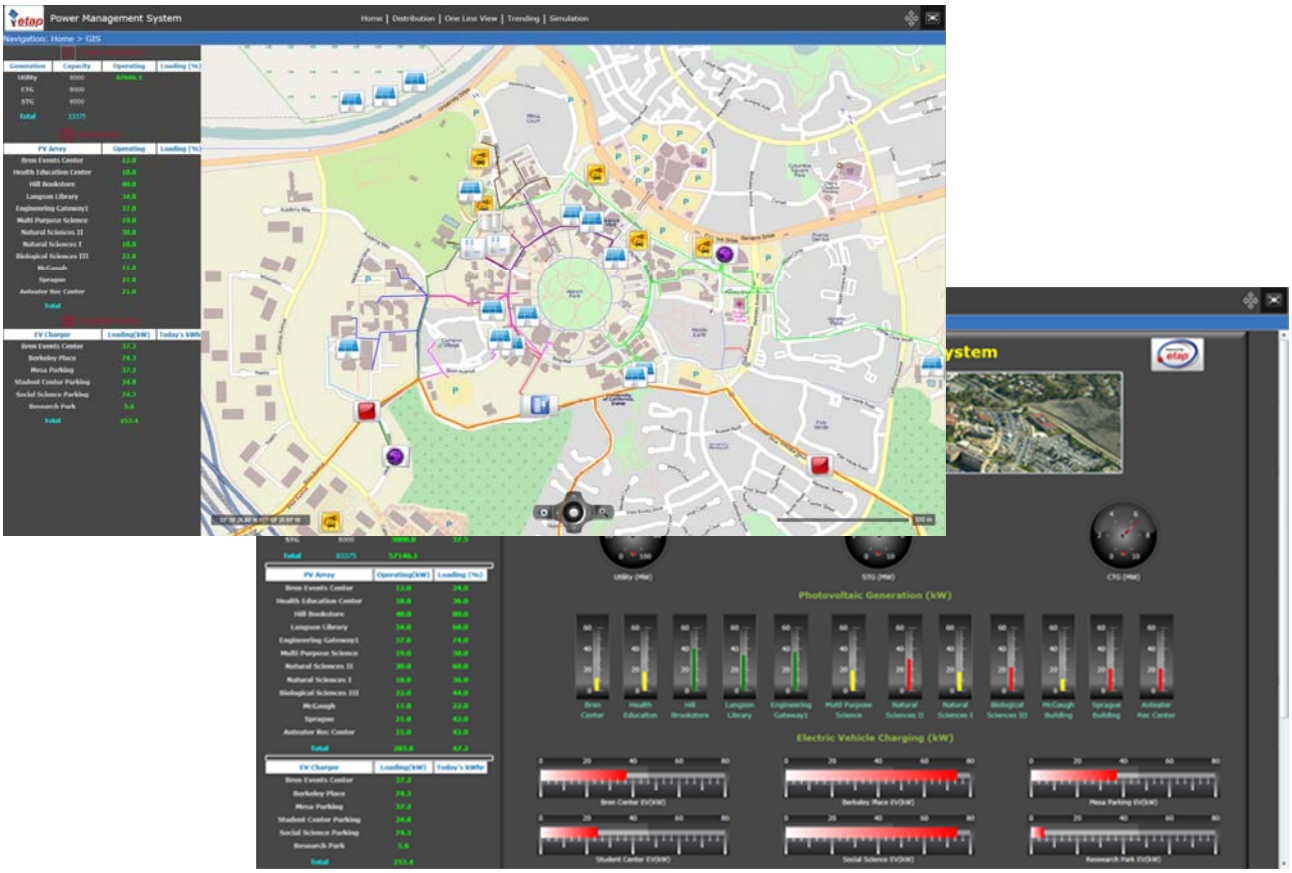

Figure 9. ETAP Software Interface for UCI Microgrid Operators.

2.5 Amonix CPV-7700 Performance

The site contains two Amonix 7700 CPV systems with a combined peak output rating of approximately 120kW. The record maximum AC power output was measured at 126.19kW at 999.94W/m^2 direct normal irradiance (534m^2 lens area), yielding an overall system efficiency of 23.63%. Each system contains a 21 x 12 module array mounted on a two-axis tracker and a Solectria 7700 PVI inverter. Temperature effects on efficiency were negligible and the system showed a power output proportional to DNI at a ratio of 147.5kW / (W/m^2) with a cut-in threshold of 350 W/m^2. Over the course of 15 months (June 2012 to August 2013) the system produced 297.4MW-h of energy which averages an output of 82.68% of the expected energy output as determined by the California Renewable Energy Transmission Initiative 2012-2013 data sources on DNI. Figure 10, Figure 11, Figure 12 show the monthly energy production compared to predicted production, peak power output, and direct normal irradiance, respectively. Amonix data acquisition devices provided uninterrupted measurements throughout the systems' operation.

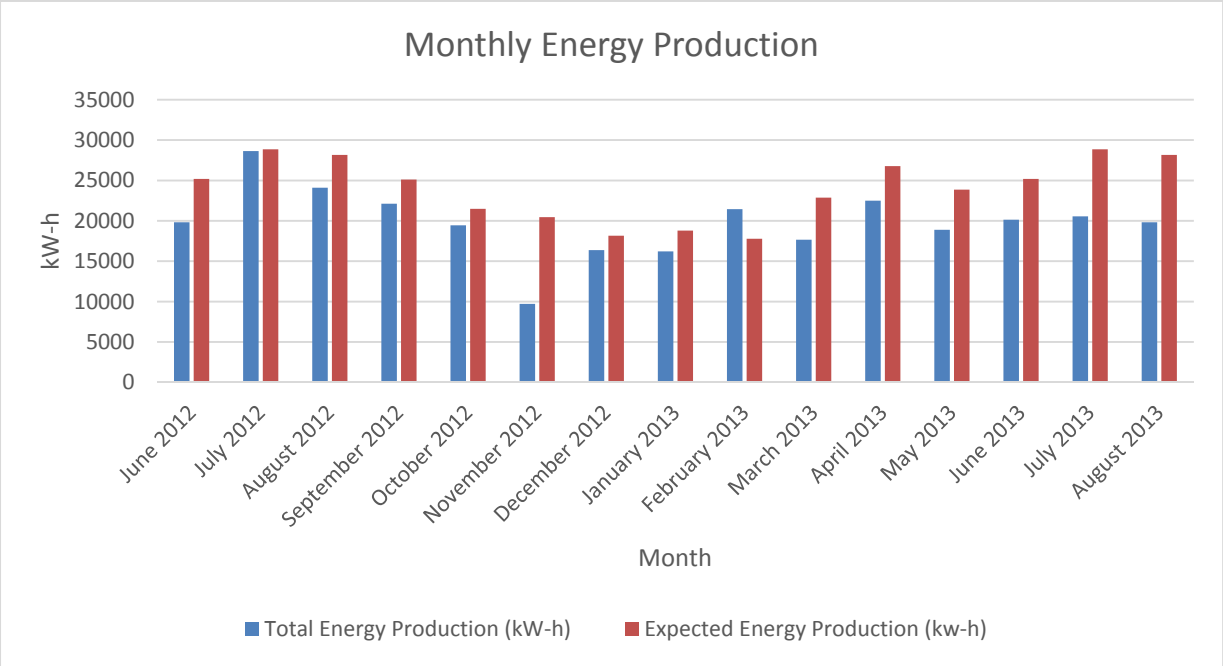

Figure 10. Monthly Energy Production.

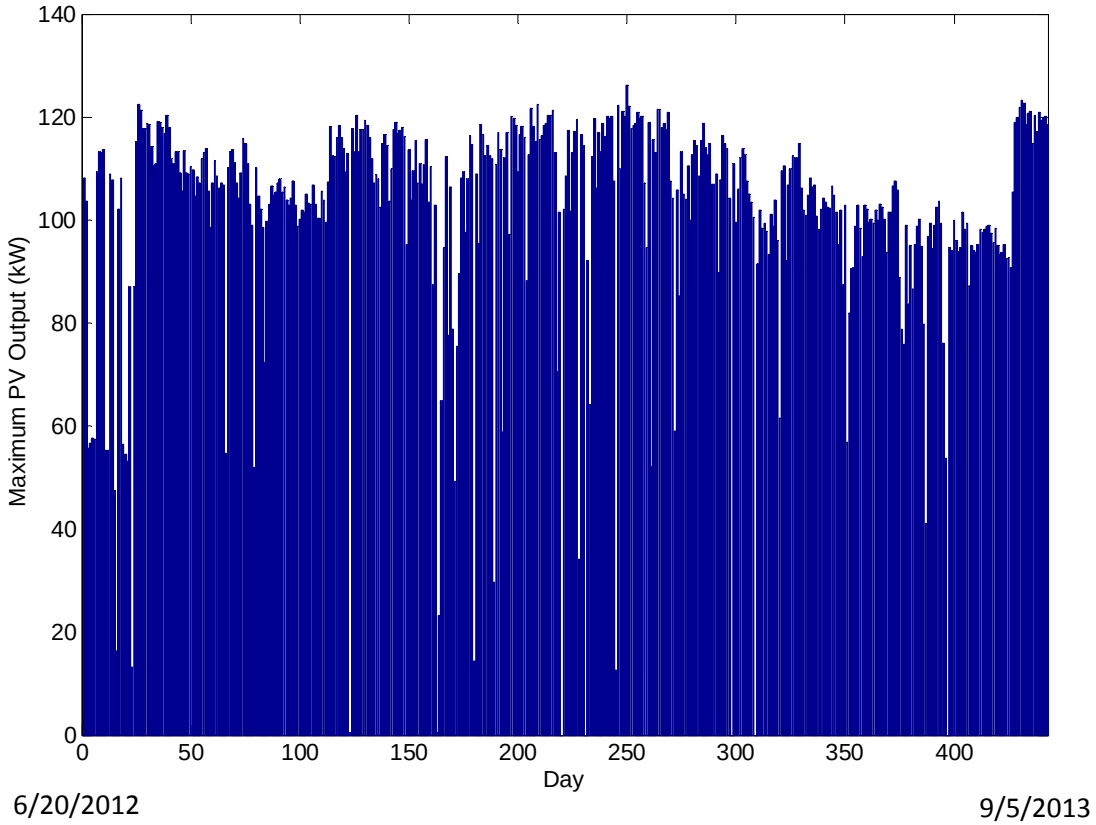

Figure 11. Peak Daily CPV Output from 6/20/2012 to 9/5/2013.

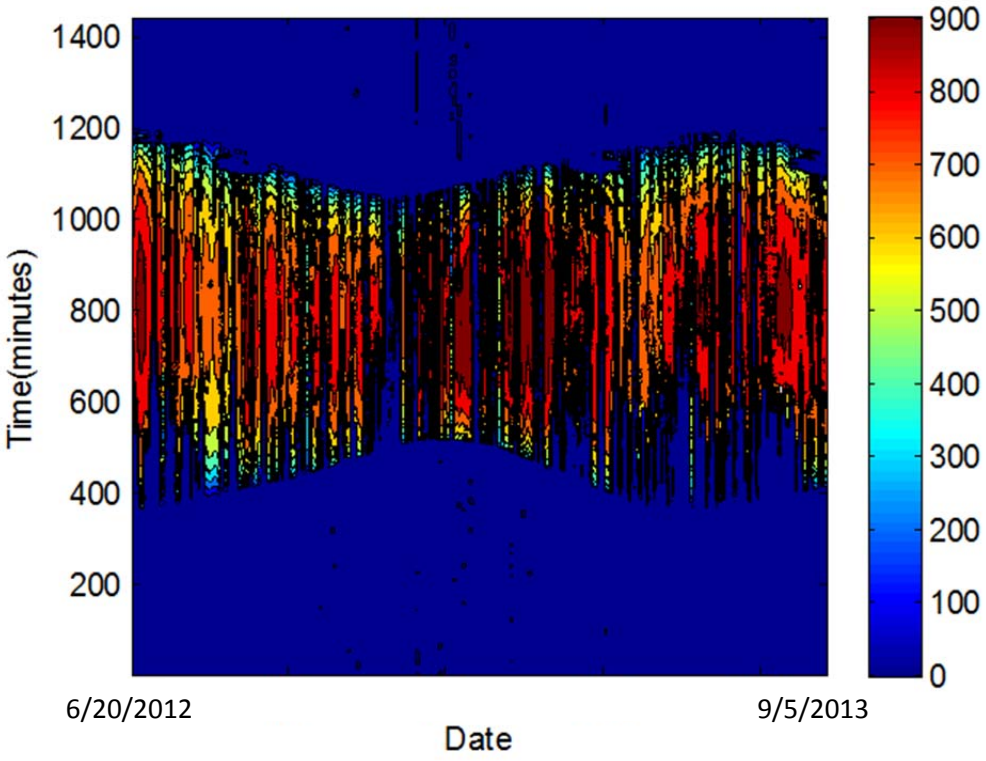

Figure 12. Direct Normal Irradiance from 6/20/2012 to 9/5/2013.

As shown in Figure 13 and Figure 14 the power output of the systems with respect to DNI and temperature are relatively constant. Outliers occur as a consequence of data interruptions or system shutdowns due to maintenance. The output power to DNI ratio has been measured at 147.5 kW / (W/m2) and an efficiency temperature coefficient of < 0.4% / degree Fahrenheit has been recorded.

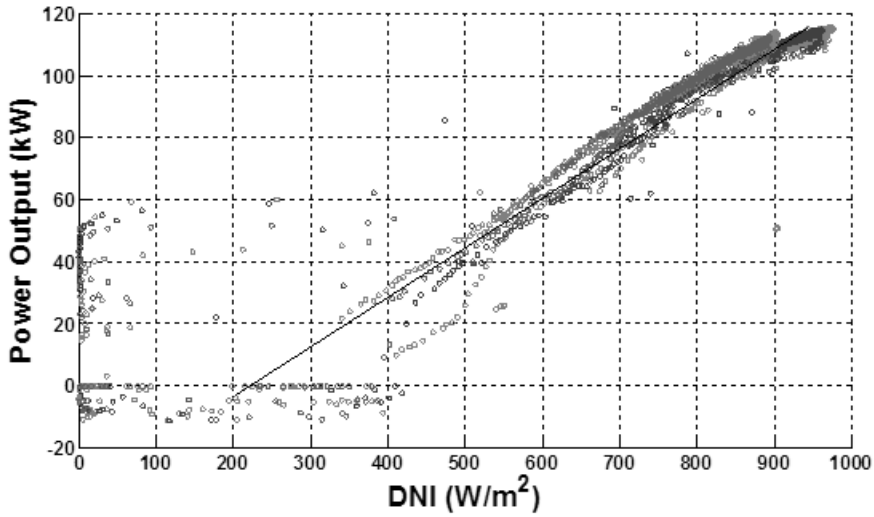

Figure 13. Power Output versus DNI.

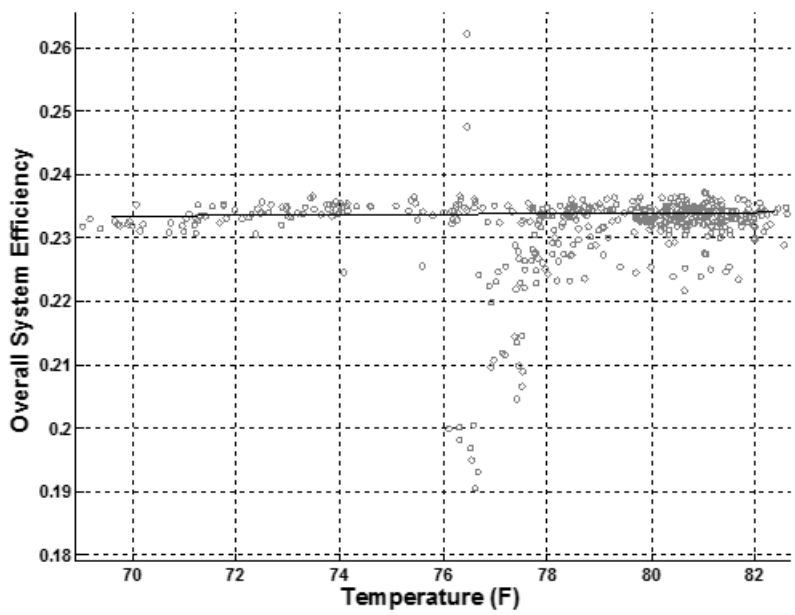

Figure 14. Overall System Efficiency VS. Ambient Temperature.

An estimate of the power spectrum was obtained via a Fourier transform of the DNI data set. The power spectrum represents the average signal power per given frequency and is a convenient way to quantify the amount of PV power variation per given timescale. In the power spectral density map shown in Figure 15, any peaks in the power spectral graph correspond to timescales of high variability. For example, the first peak that occurs at approximately 10^-1.915 mHz (1 cycle per 24 hours) corresponds to the variability that occurs due to the diurnal cycle.

Other peaks occur at 10^-1.633 mHz (11.95 hours), 10^-1.464 mHz (8.1 hours), 10^-1.338 mHz (6.04 hours), 10^-1.239 mHz (4.82 hours), and 10^-1.115 mHz (3.968 hours). Beyond the 3.968 hour timescale, intermittency shows no predictable cyclic behavior.

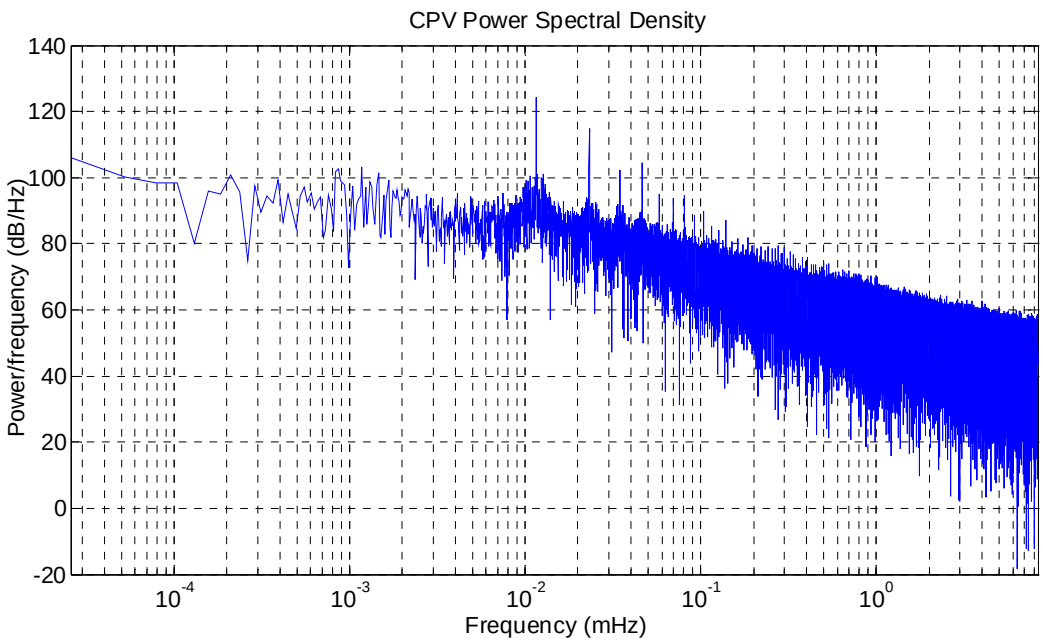

Figure 15. CPV Power Spectral Density

Table 3. Timescale to Frequency Conversion.

Timescale	Frequency (mHz)	Frequency ($\log_{10}$)
1 Second	1000	3
1 Minute	16.66667	1.221849
1 Hour	0.277778	-0.5563
1 Day	0.011574	-1.93651
1 Week	0.001653	-2.78161
1 Month	0.000386	-3.41363

2.5.1 Summary of Amonix CPV-7700 Performance

- Overall system efficiency was measured at 23.63%. The power output to DNI at a ratio was measured at 147.5kW / (w/m^2) with a cut in threshold of 350 W/m^2.
- Ambient temperature showed negligible effects on system efficiency.
- Over the course of 15 months (June 2012 to August 2013) the system produced 297.4MW-h of energy.
- The Amonix installation at UCI performed well in summer months but suffered reduced

energy production due to cloud cover and costal region fog during winter and early spring months. During November 2012, energy production dropped to 47.5% of expected values. Over the course of 15 months the installation produced 83.2% of expected energy.

- Power output intermittencies are unpredictable from historical DNI data alone beyond the 3 hour timescale.

3 Campus Electric System Operation with CPV Resources

3.1 Model Development

Two simulation packages were used in parallel to study the impact of the Amonix CPV-7700 systems on the UCI circuit: ETAP and MATLAB. In both simulations, data from the Melrok and Amonix systems are used as inputs into the circuit models. The dual simulation approach was selected as it allows for the campus wide traditional load flow studies (ETAP) and detailed sub-circuit and investigational simulations (MATLAB/Simulink).

3.1.1 Circuit Model

A dynamic load flow model was developed in ETAP taking into account the circuit topology, line and transformer impedances, and system loads. Specific to UC-9, the Amonix system is connected to the Anteater Recreation Center motor control center (ARC-MCC) via 1100’ of 3 350MCM conductors in a 3” conduit. The ARC, in turn, is connected to the UCI substation switchgear via a 2MVA 12kV to 480V transformer (Z = 5%, X/R = 7.29) and 11235’ of cable (Z = 0.05078 / 1000’, X/R = 1.482). Figure 16 shows the ARC/Amonix portion of the UC-9 one-line diagram. Using one-line diagrams provided by facilities management, the UCI electrical distribution system including subcircuits UC-1 to UC-10 were imported into the ETAP circuit model allowing for load flow simulations of the entire UCI electrical system. Similarly, an identical MALAB/Simulink model was also developed with the same circuit parameters. The MATLAB/Simulink model allow for the rapid development and testing of experimental control algorithms and circuit devices.

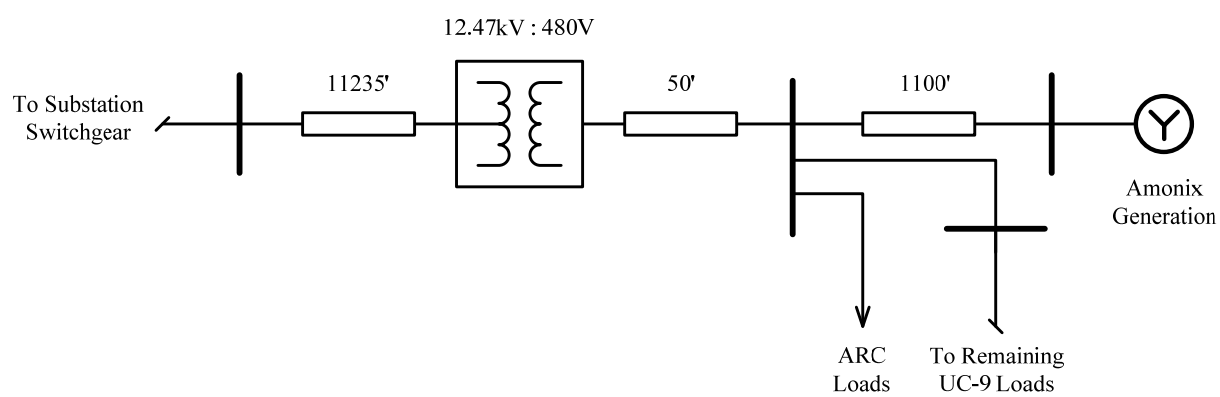

Figure 16. Amonix / UC-9 Oneline Diagram Overview.

Baseline simulations were conducted and results were compared against field voltage measurements to verify the models. The ETAP model accepts substation voltage, ARC load, and Amonix power data as inputs and outputs simulated voltage profiles of the ARC and Amonix busses. Due to the current unavailability of 12kV substation voltage measurements, the substation voltage profile was approximated by scaling the voltage profile measured at the Multipurpose Science & Technology Building (MSTB): a building near a 12kV bus. It was noted that throughout the UCI microgrid, recorded 12kV voltage profiles were nearly identical with the exception of a slight scaling factor, indicating that any variations in 12kV bus voltages were primarily due to utility fluctuations and not local load effects. Additional 12kV loads downstream of the ARC were also approximated has having negligible impact on the 480V ARC-MCC local voltage profiles. These loads include the Verano Place graduate housing, Social Ecology, and Social Sciences loads. 480V voltage profiles at busses downstream of ARC-MCC were, however, largely affected by local loads and generation. In Figure 30, measured voltage profiles at the ARC-MCC and at the Amonix terminals are shown. The local voltage rise seen at the Amonix terminals is attributed to the series impedance in the 1100' cable connecting the panels to the ARC-MCC, and the slight depression in the ARC-MCC voltage profile is due to the reactive power consumption at the bus.

3.1.2 CPV Model

Two models were developed to simulate the Amonix 7700 system; a load flow model and a transient model. In the load flow model, CPV systems are modeled as negative three phase, three-wire dynamic loads. In this model, active power and reactive power are injected as a function of a control signal and the line voltage. Measured power output data from the Amonix power meters were used as the control signal in baseline studies. Later, these values were modified to simulate the effects of additional Amonix systems on the UCI circuit. The following equation describes the injected current to power and line voltage relationship:

$$I_{rms} = \frac{P_{measured}}{\sqrt{3} * V_{L-L}}$$

It was noted that CPV power output was linearity proportional to direct normal irradiance, with a proportionality constant of 150W per W/m^2 and a cut-in of 350W/m^2. While this allows the current injection in the above equation to be expressed in terms of line voltage and DNI, as direct power measurement data were available, use of kW output vs DNI input was selected as it automatically accounts for inverter inefficiencies. The load flow model converges rapidly at steady-state solutions and is used to simulate over large timescales such as days or weeks.

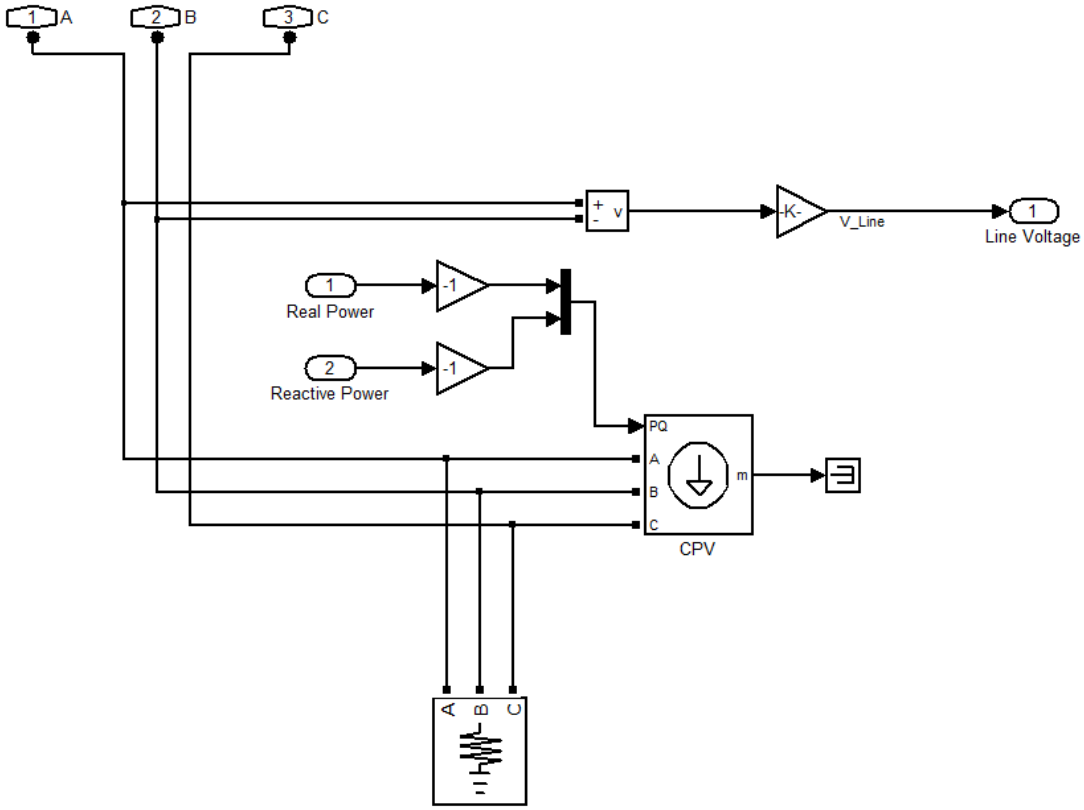

Figure 17. CPV Load Flow Model.

A transient model was also developed in MATLAB/Simulink to investigate the effects of events such as passing cloud cover, voltage sags, sudden load switching, and faults. In this model the controller dynamics of the inverter are taken into consideration. The CPV modules are assumed to be operating at the maximum power point and are modeled as voltage sources. A DC link decoupling capacitor buffers the input voltage before being inverted by a six switch, three phase DC-AC inverter block. In the internal controller, a current controller modulates the duty cycle of the active switches to synchronize the inverter output with the grid, control power output, and stabilize the operation of the inverter while low-pass filters reduce output ripple. Here, an abc/dq transform is applied and proportion-integral controllers are utilized to generate the switching patterns required to control the active switches of the power stage. The power stage consists of six pulse width modulated high frequency MOSFET switches. Finally, an dq/abc transform is applied and two external loop proportion – integral controllers provide feedback tracking for real and reactive output power. Figure 18 shows the components of the transient inverter model.

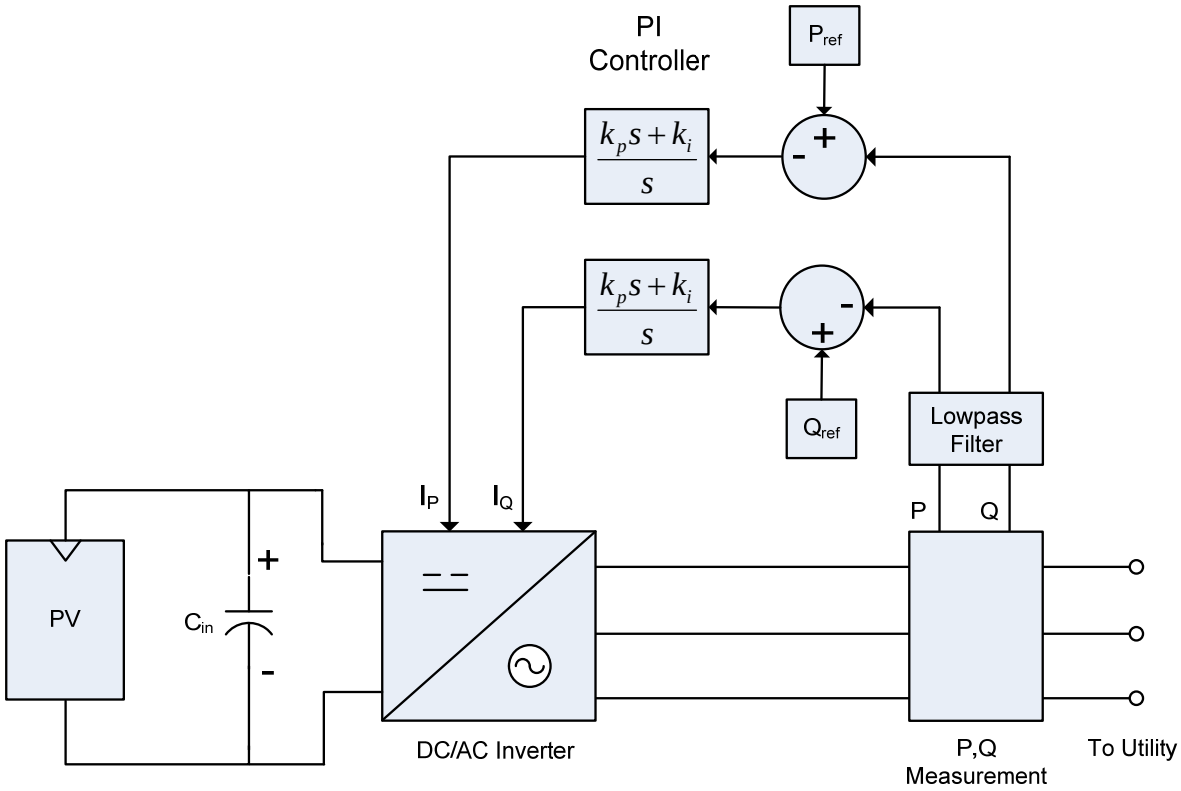

Figure 18. Dynamic CPV Inverter Model.

Figure 19 shows dynamic CPV simulation results for an inverter step demand of 35kW (15kW to 40kW). The real power output shown in blue is commanded to increase at t = 0.4 s and decrease at t = 1s. The reactive power output is set to maintain 0 VAR. The system is able to accurately track the reference signal, however temporary transients occur as reactive power feedback loop attempt to track against real power step changes, resulting in temporary reactive power injection. Such step changes might occur during sporadic cloud cover.

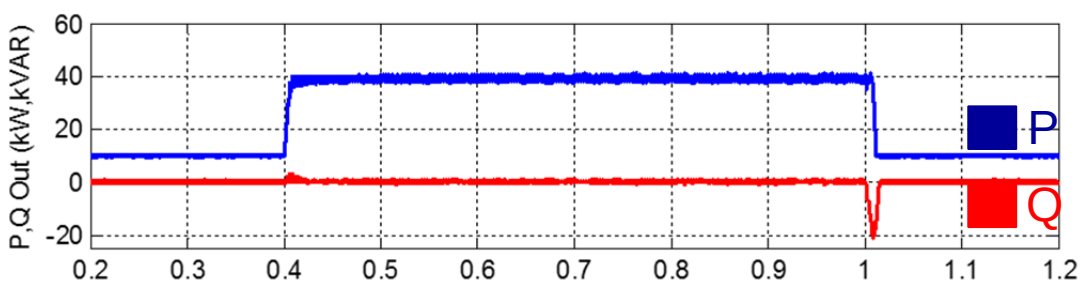

Figure 19. Dynamic CPV Model Real and Reactive Power Tracking.

3.1.3 Building Load Model

Similar to the CPV model, building loads are modeled as dynamic variable loads (current

sinks as opposed to current sources). Unlike the CPV model, building loads may sink both real and reactive power (the Amonix CPV-7700 systems are configured to operate at unity power factor, so the reactive power output setpoints are fixed at zero). Archived Melrok meter data is fed into the building load models via the real and reactive power data ports and the dynamic load component adjusts current and current phase according to line voltage to sink the appropriate amount of real and reactive power. For buildings at which Melrok meter data was unavailable, the building load profile was approximated by scaling the subcircuit load profile. Factors used to determine the scaling factor include building type, building square footage, internal building loads, and transformer nameplate ratings.

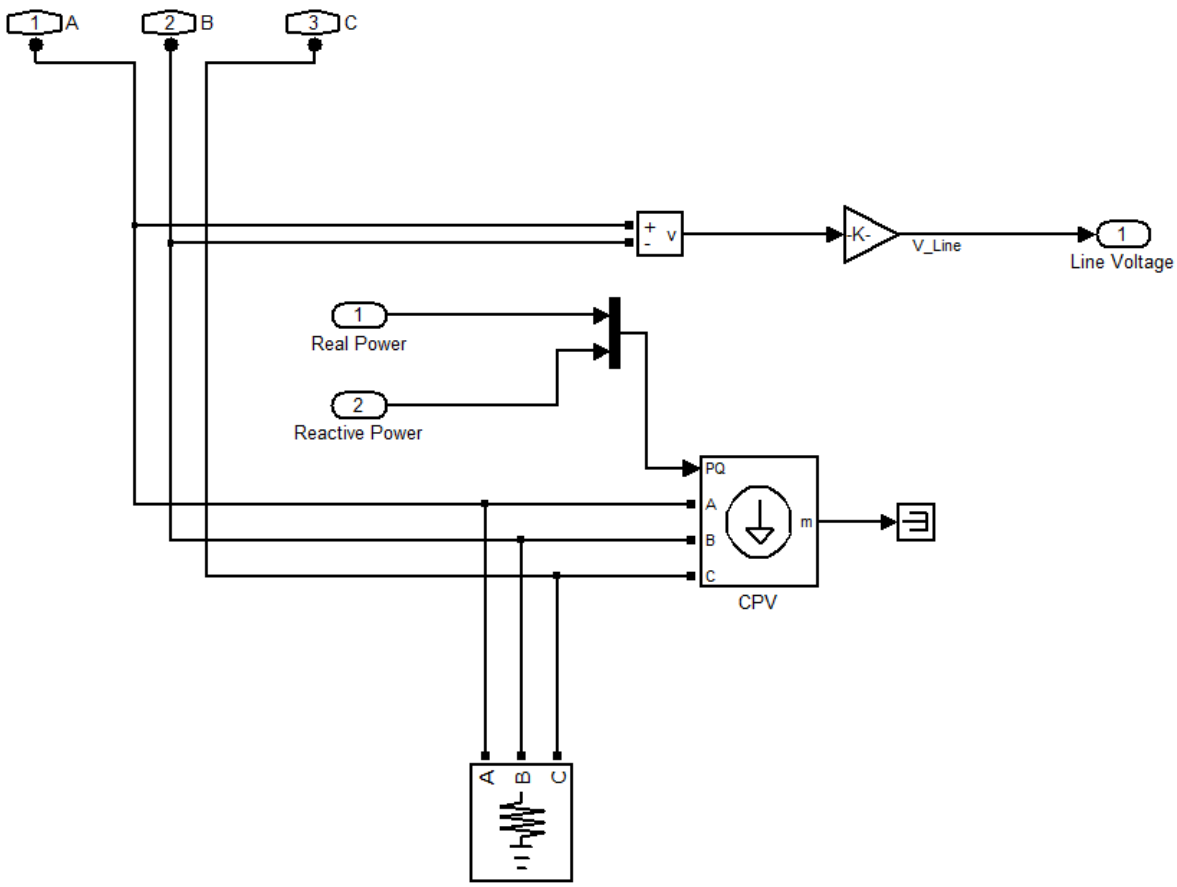

Figure 20. Building Load Model.

3.1.3.1 Model Validation

To validate the ETAP/Simulink models, real and reactive power generation data from the Amonix system and real and reactive load data from the Melrok ARC meters were input into the UC-9 sub-circuit model. The resulting voltage profiles from the simulation were compared with measured bus voltages from the field devices. Model parameters such as line and transformer impedances and inverter efficiencies were tuned using a least-squares estimator to minimize the overall difference in simulation voltage profiles to measured voltage profiles. This process was

repeated throughout the entire campus model. The acceptable tuning criteria was set at a 5% RMS error and it was noted that the majority of the provided one-line diagram values were accurate to this criteria. In the tuning process, resistance values are modified while original X/R ratios are kept constant for 480V line segments. Reactance values are modified and X/R ratios are kept constant for 12.47 kV and 66 kV line segments. Transformer parameters are assumed to be correct.

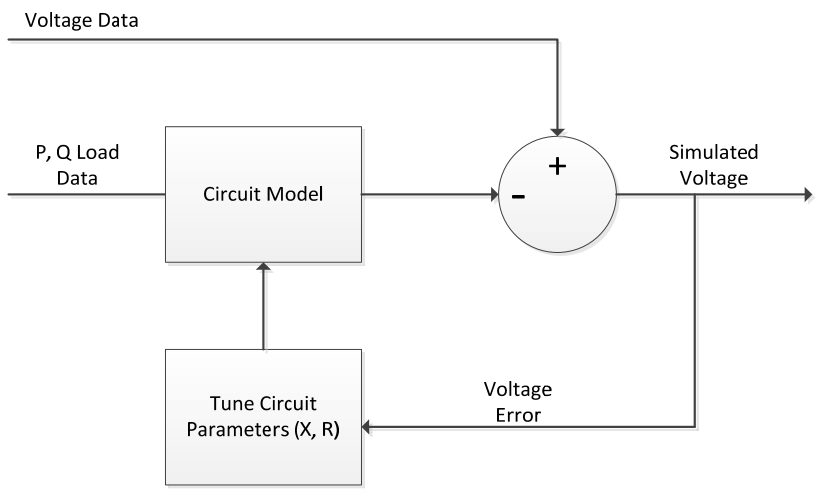

Figure 21. Circuit Model Parameter Tuning Procedure.

Due to a lack of 12kV substation voltage data, the 480V bus voltages from the Melrok system were scaled to 12kV and used in substitution. It was noted that throughout the UCI electrical network all recorded 480V bus voltage profiles were similar indicating that the overall profile shape is attributed to the profile of the 12kV feeders as opposed to local loading and CPV generation effects. Figure 22 illustrates the similarity in the voltage profile across various UCI buildings, indicating a strong substation voltage influence. Figure 23 and Figure 18 show comparisons of measured and simulated voltage profiles after model tuning at the ARC MCC and Amonix system, respectively. ANSI Range A voltage limits and inverter overvoltage limits are shown as well. Root mean square error across an entire 24 hour simulation run has been noted be less than 5% after model tuning.

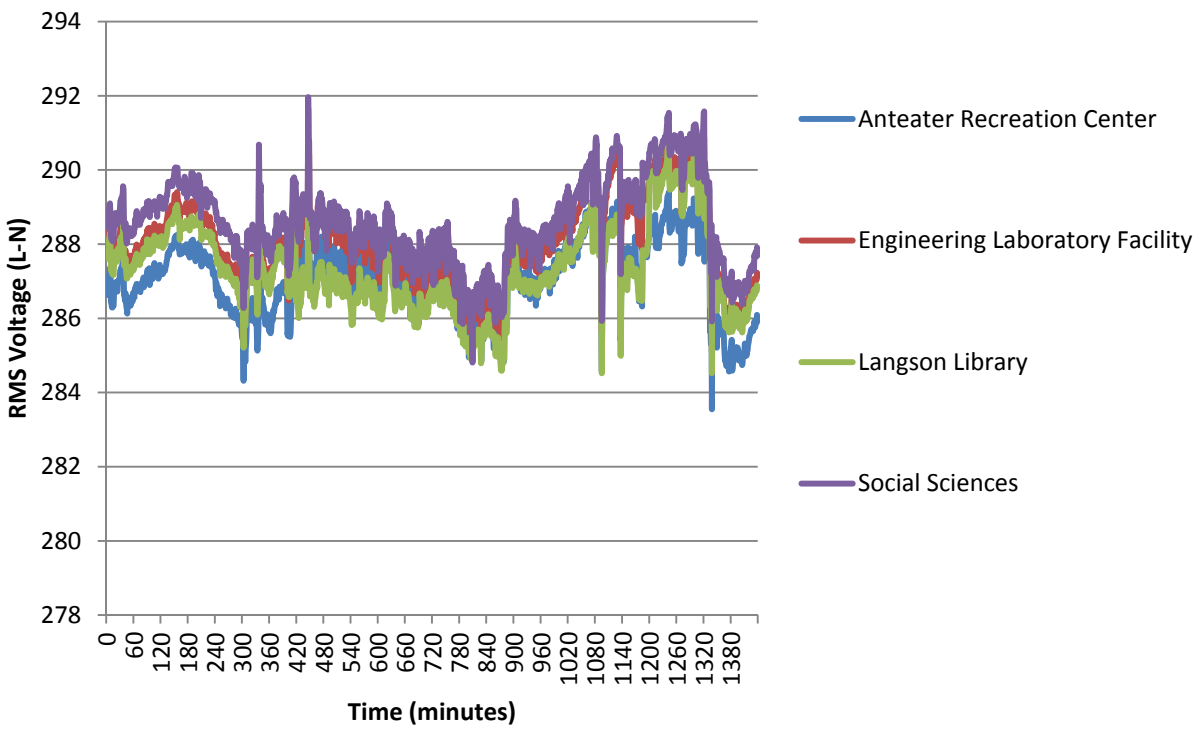

Figure 22. Voltage Profiles of Various UCI Buildings.

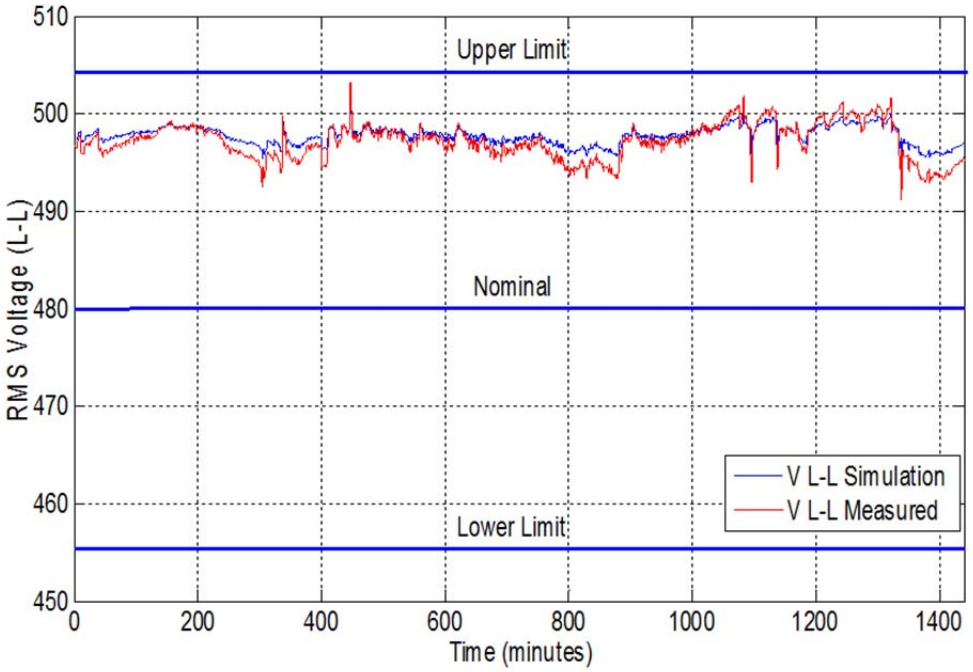

Figure 23. Baseline ARC MCC voltage profiles. 8/28/2013.

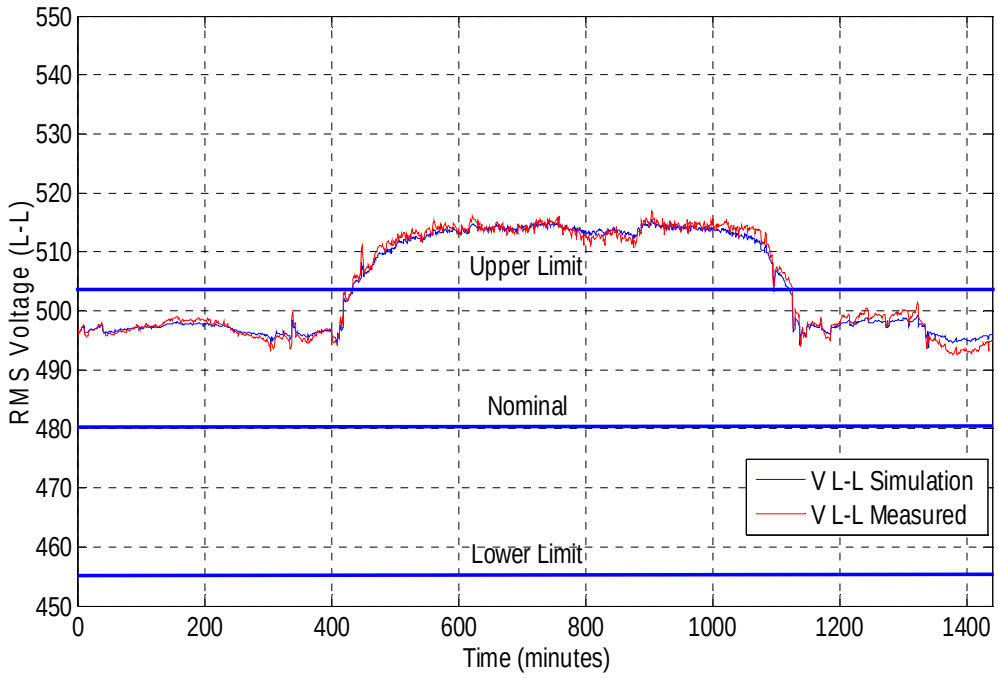

Figure 24. Baseline Amonix Voltage Profiles. 8/28/2013.

3.2 Analysis and Results

Three analyses were performed: 1) evaluation of the impact of the current solar resources (fixed PV and CPV) impact campus operation, 2) evaluation of the impact of the current Amonix systems on the UC-9 circuit, and 3) evaluation of the impact of increased penetrations of CPV systems on the UCI distribution system.

3.2.1 Impact of Current Solar Resources on Campus-wide Operation

Historical generation and demand interval data from 2011 and 2012 of the UC-9 circuit operating without the Amonix system installed provided by facilities management were used to establish representative high demand and low demand scenarios for the UCI circuit. These representative demand profiles are then used as simulation inputs for further studies on the impact of high penetration CPV on the UCI distribution circuit. The profile depicted in Figure 25 and Figure 26 show the profiles selected for winter and summer months, respectively. Other data used include SCE import, gas and steam turbine output, and existing flat plate solar output. As seen in Figure 25 and Figure 26 on-campus turbine generation variability is considerably high in winter months due to heating demands while in the summer the gas turbine generator is typically operated near maximum capacity continuously.

The coincidence of solar energy production with campus wide electricity demand patterns is well established for winter demand, during which existing PV satisfies approximately

3% of peak demand. During summer months, peak solar generation precedes peak electrical demand by approximately an hour. The peak demand reduction due to currently installed PV generation during the summer increases to approximately 4%.

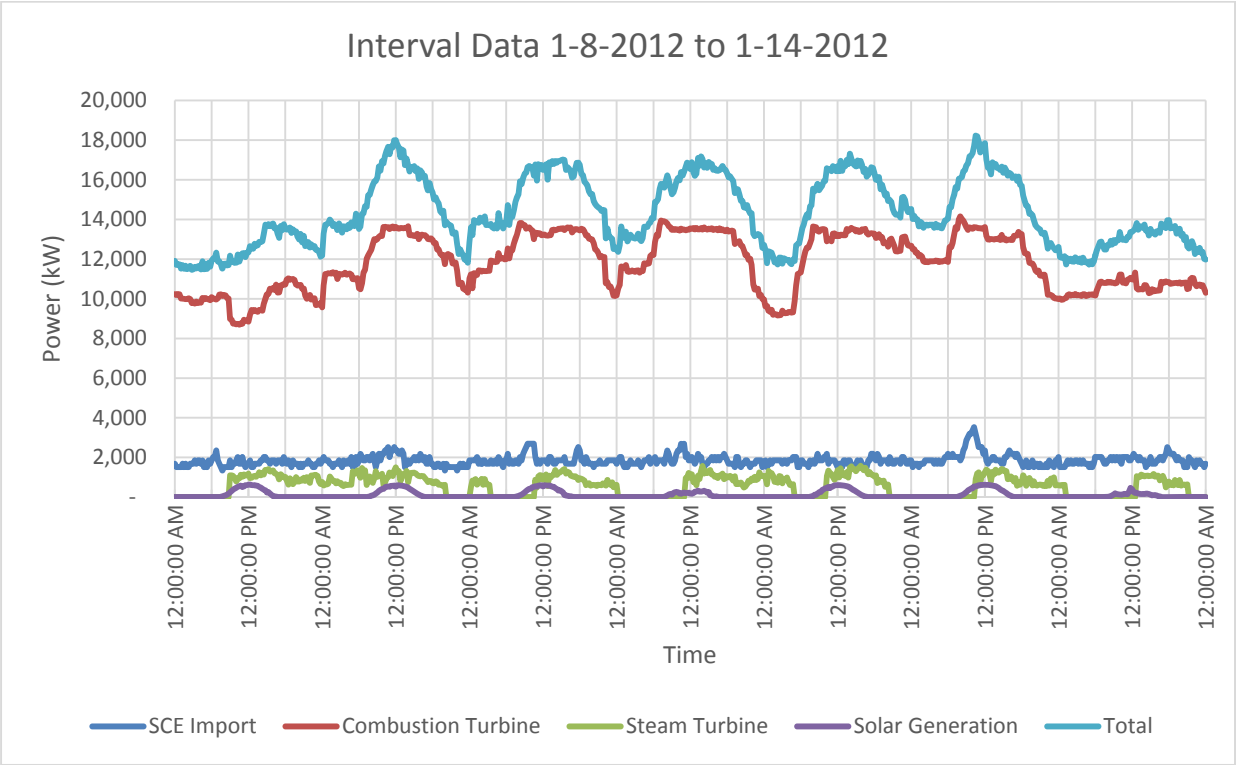

Figure 25. Representative Winter Load Profile.

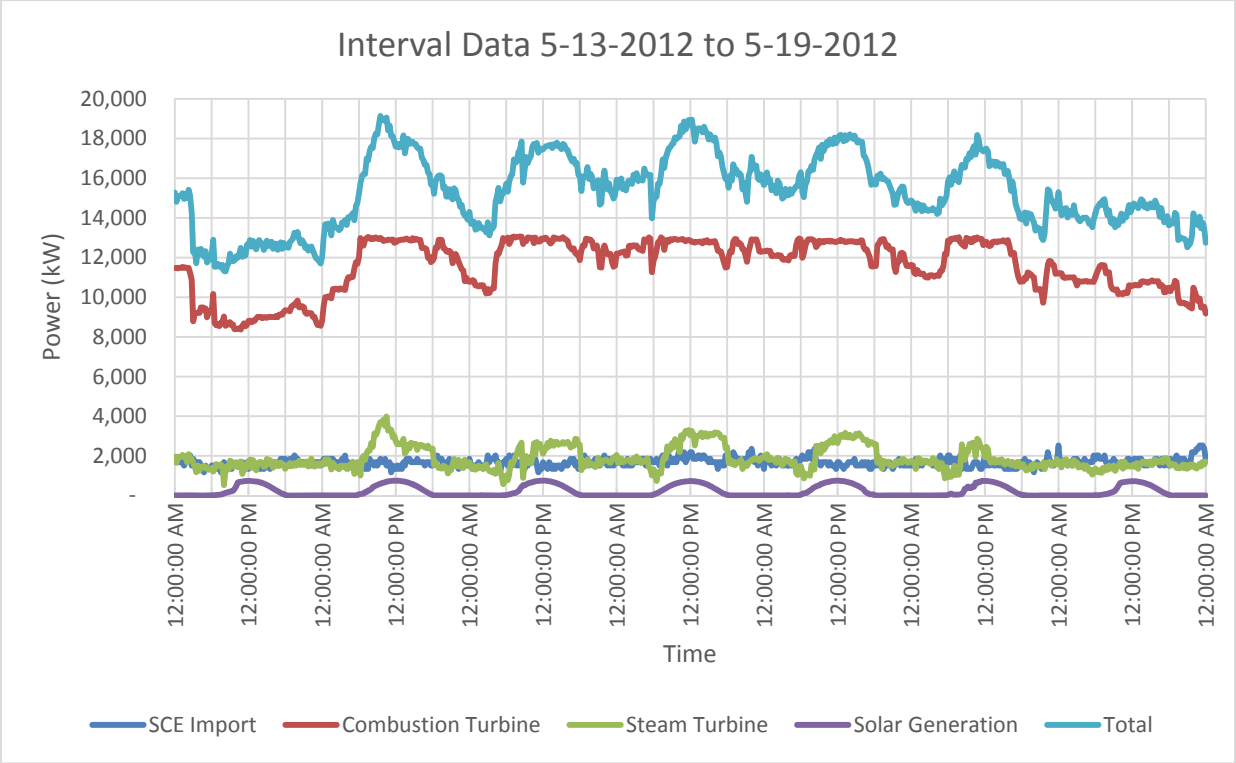

Figure 26. Representative Summer Load Profile.

Particular attention is given to meeting campus load while operating with a 1 MW minimum import restriction. This is met by operating at an additional 1MW safety margin and high penetration solar installations coupled with the minimum gas turbine generator turn-down limit of 8 MW may possibility push the SCE import below the 1MW level. As shown in Figure 27 and Figure 28 the campus may only accept up to 3.151 MW of total solar generation without solar curtailment capabilities or additional load before the 1MW import limit can no longer be met. Increasing PV penetration without increasing campus load would increase the risk of requiring a shut-down of the turbine generator, or falling below the 1MW import requirement.

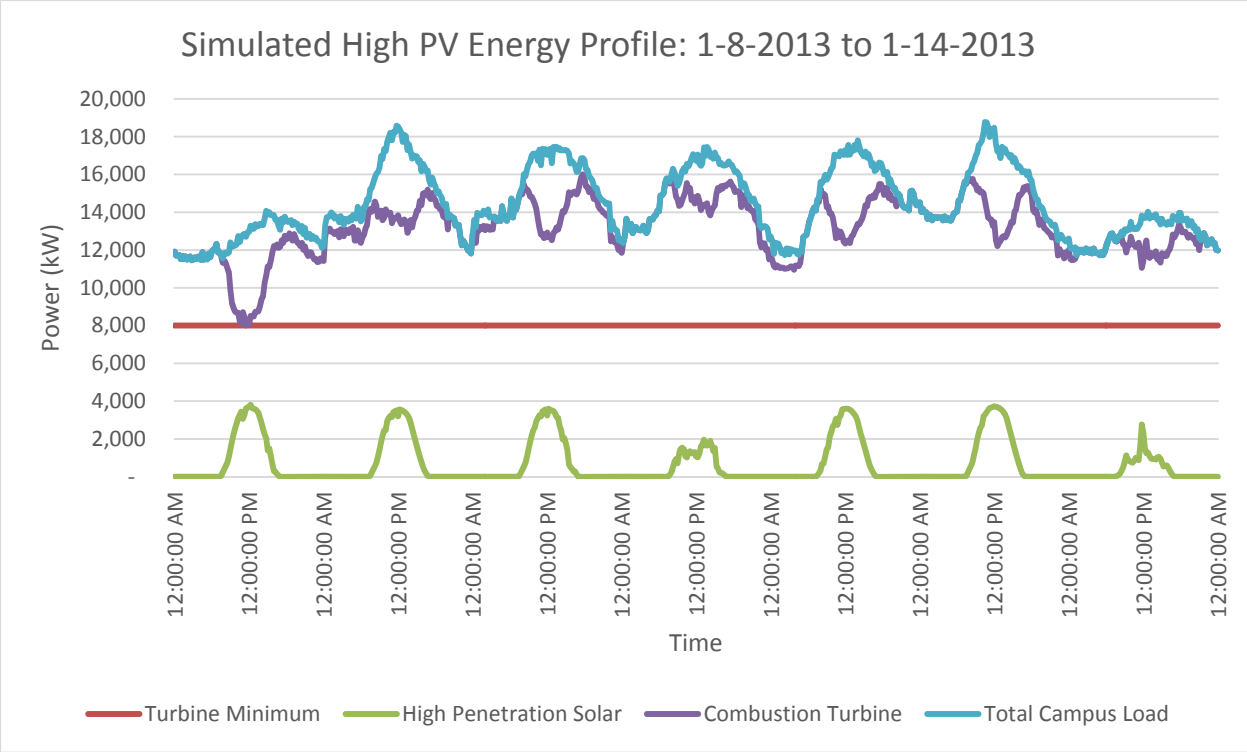

Figure 27. Effects of High PV Integration on the Winter Campus Energy Profile.

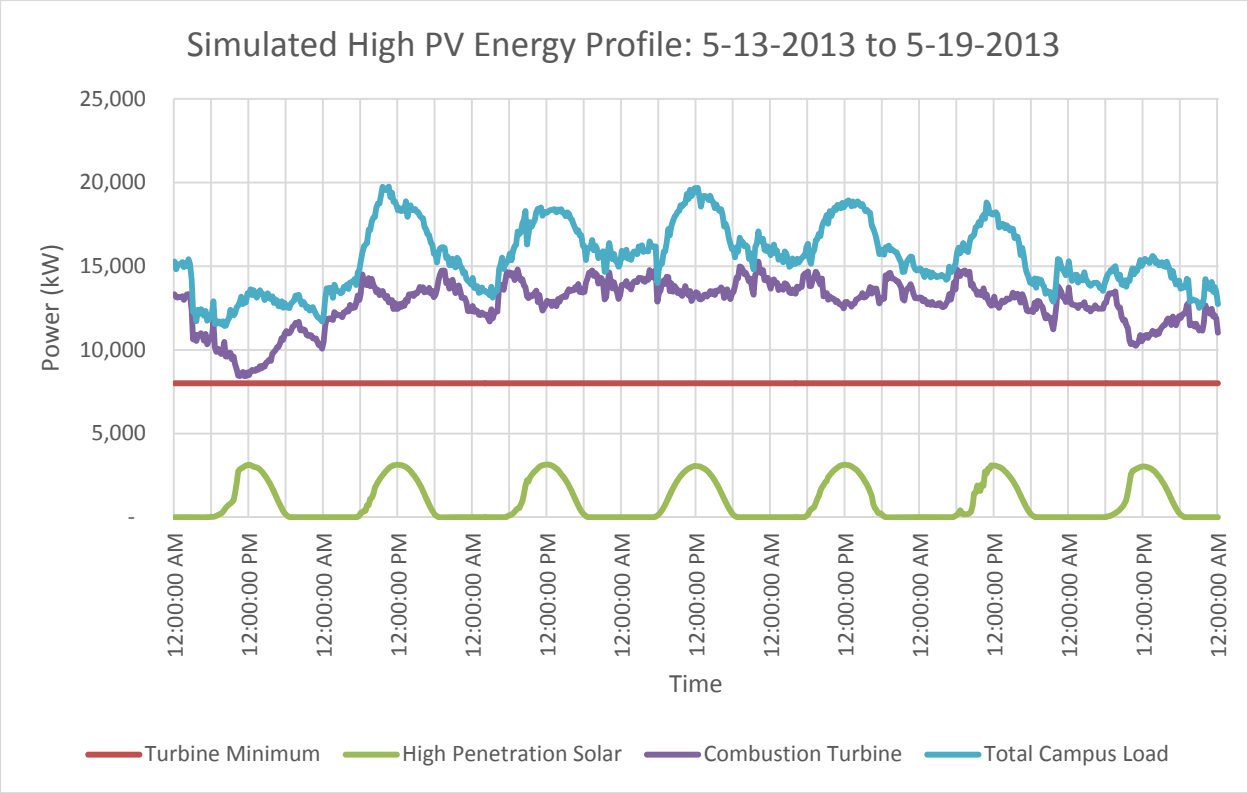

Figure 28. Effects of High PV Integration on the Summer Campus Energy Profile.

3.2.1.1 Summary

- Maximum allowable PV generation without curtailment or energy storage capabilities while meeting minimum import requirements has been established at 3.151 MW.
- Solar generation coincides with demand during winter months and precedes demand by approximately 1 hour during summer months.
- Approximately 4% of peak campus load is supplied by currently installed PV. This amount may be increased to 13.1% while staying within minimum import requirements.
- Overall campus average electricity consumption is approximately 14 MW for winter months and 15 MW for summer months. Winter weekend loads peak at approximately 77% of peak weekday loads and 83% for summer months.

3.2.2 Impact of Amonix CPV System onUC-9 Circuit Operation

In this scenario, data from the Amonix installation and Melrok ARC-MCC meters are used to characterize the performance of the CPV-7700 system and analyze the impact of the installation on the UC-9 subcircuit. The systems' Solectria 7700 inverters output unity power factor AC into the distribution circuit at the ARC-MCC with a real power output proportional to direct normal irradiance. The system performance, impact on the UC-9 bus voltages, and impact of solar intermittency are analyzed. The Amonix panels are connected to the main bus of the student recreation center which represents an electrical load of approximately 300kW to 500kW, and further connected to the UC-9 distribution circuit via a 2MVA transformer. As the resulting penetration factor may be as high as 40% for the ARC and approximately 1.54% for the UC-9 sub-circuit, assuming normal transformer loading conditions, particular attention is paid to the impact of the CPV-7700 system on local bus voltages and the voltages at the Amonix inverter terminals to ensure that voltage limits are not exceeded. Data from these studies were used to validate the UCI one-line model parameters. Comparisons are made of UC-9 operation with and without the CPV-7700 systems and the performance of the CPV-7700 systems are reviewed. Figure 29 shows an example power profile at the ARC-MCC with the Amonix system installed. Amonix power production results in a large decrease in net power consumption.

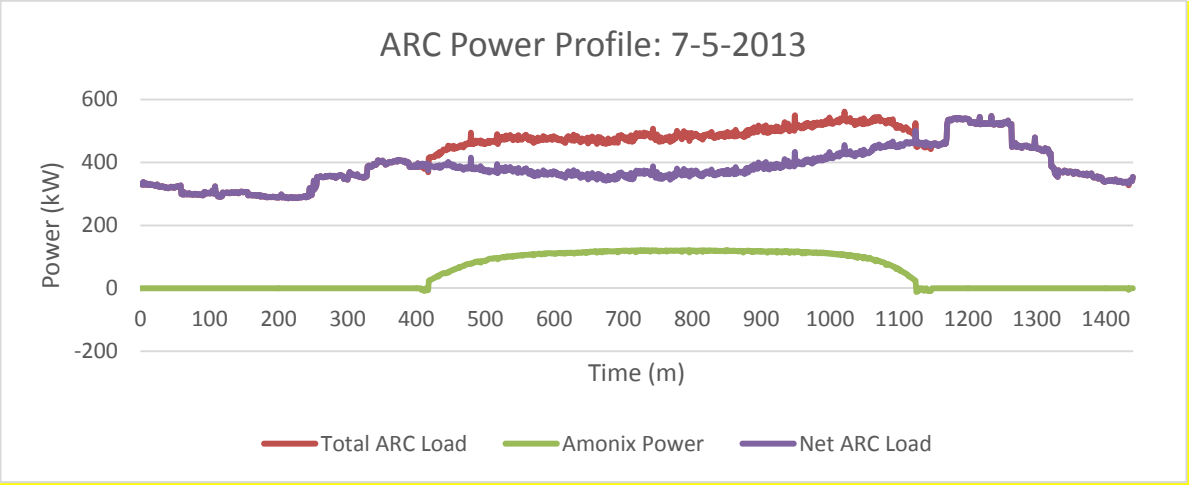

Figure 29. Example ARC-MCC Power Profile.

3.2.2.1 Impact on UC-9

The addition of the Amonix CPV 7700 systems results in significant load reduction on the UC-9 ARC circuit. At peak solar production, total local load demand is reduced by up to 40% and the impact on local bus voltage should be considered. Measured voltage profiles from the MelRok system show minimal voltage profile disturbance at the ARC-MCC bus, but substantial voltage rise at the Amonix systems' inverter terminals. Additionally, above nominal line voltages per ANSI range A utilization voltage limits were noted throughout the UCI system, though this is likely a consequence of the operation of the UCI electrical network and not the Amonix installation or other PV generation. Voltages increase at the ARC terminals due to real power injection, and decrease at the ARC MCC due to the reactive power effects attributed to the line reactance between the inverters and the ARC MCC. As seen in Figure 30, Amonix inverter and ARC-MCC voltages are identical minus a slight voltage drop due to the line impedance between the two busses during non PV production hours and immediately diverge when power production occurs. Voltage collapse calculations show that with the currently installed conductor between the ARC and the Amonix inverters, ampacity limits are reached before the voltage collapse limit is reached. When ampacity limits are reached at 400kW the critical angle is 4.56 degrees between the inverters and the ARC-MCC.

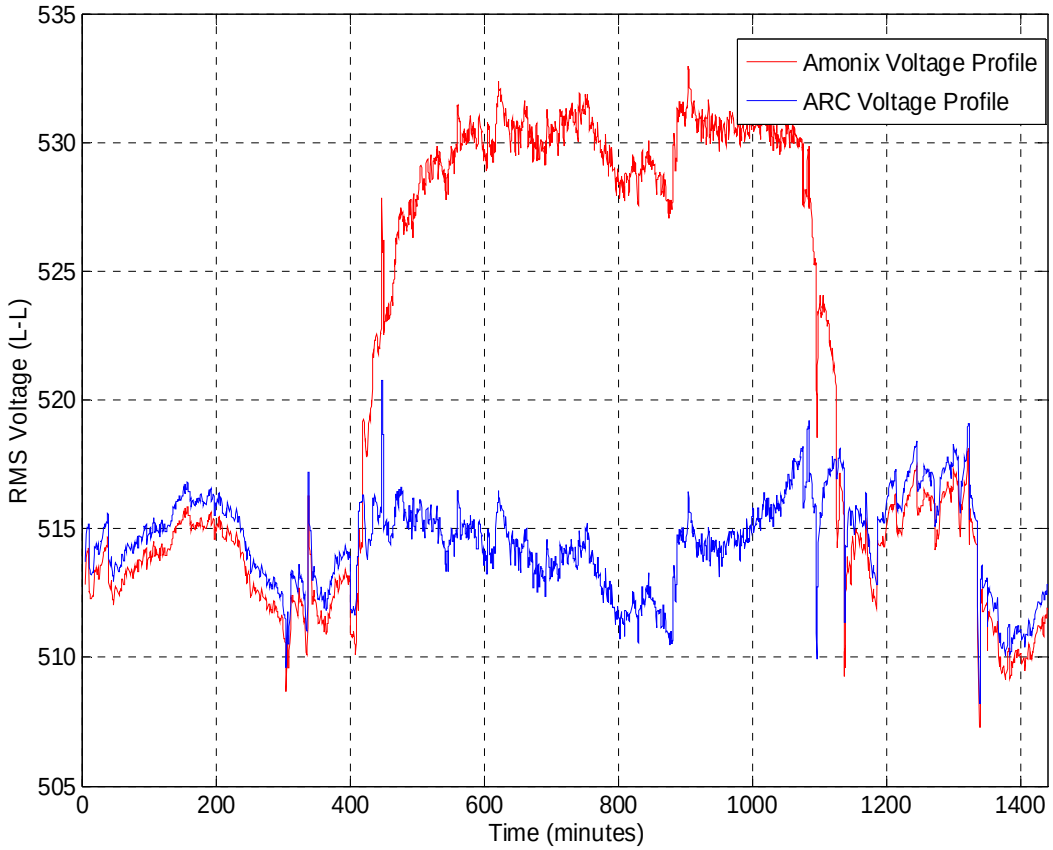

Figure 30. Amonix and ARC Measured Voltage Profiles. 8/28/2013.

3.2.2.2 Impact of Intermittency

The intermittency of solar energy presents challenges to the integration of PV resources into the UCI Microgrid. Characterizing the behavior of solar availability is crucial to maximizing the contribution of PV. Solar irradiance (direct normal, diffuse horizontal and global horizontal) and temperature data have been collected over a period of 443 days and counting from an on-site meteorological station and are used to trend the solar availability at UCI. Figure 31 to Figure 34 illustrate the intermittent nature of solar PV in a coastal region. Power production begins when DNI levels exceed approximately 250W/m2. Solar intermittency reduces power production significantly during winter months, with some months generating less than 50% of expected energy production. Overall, the Amonix installation at UCI has produced 83.2% of expected energy production as per NREL solar prospector data sets with a high in February 2013 at 120.05% and a low in November 2012 at 47.5% of expected monthly production. Intermittency effects have shown no detrimental effects such as flicker or voltage sags on the voltage profile due to the relatively stiff connection to the university substation. Figure 33 is a chart illustrating the effect of cloud cover on energy production. Green sections correspond to days in which >80 % of anticipated energy production as per NREL solar database values are achieved. Yellow days correspond with days that produced between 50% and 80%, and red blocks highlight days

in which 0% to 50% of anticipated energy is generated.

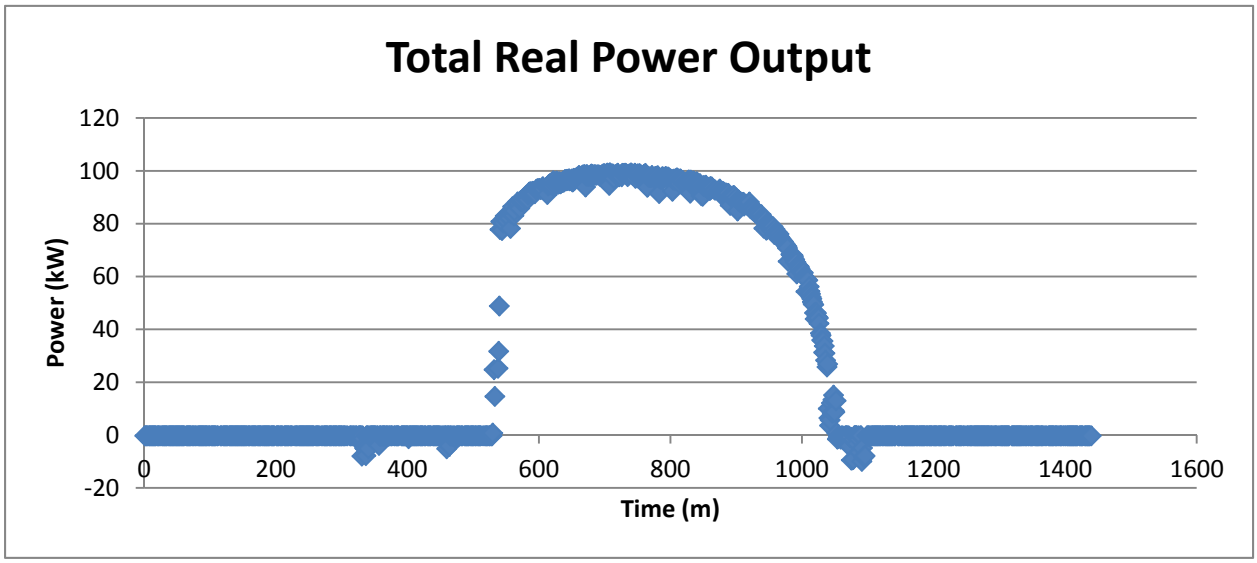

Figure 31. Typical Power Output Trend in the Absence of Intermittency.

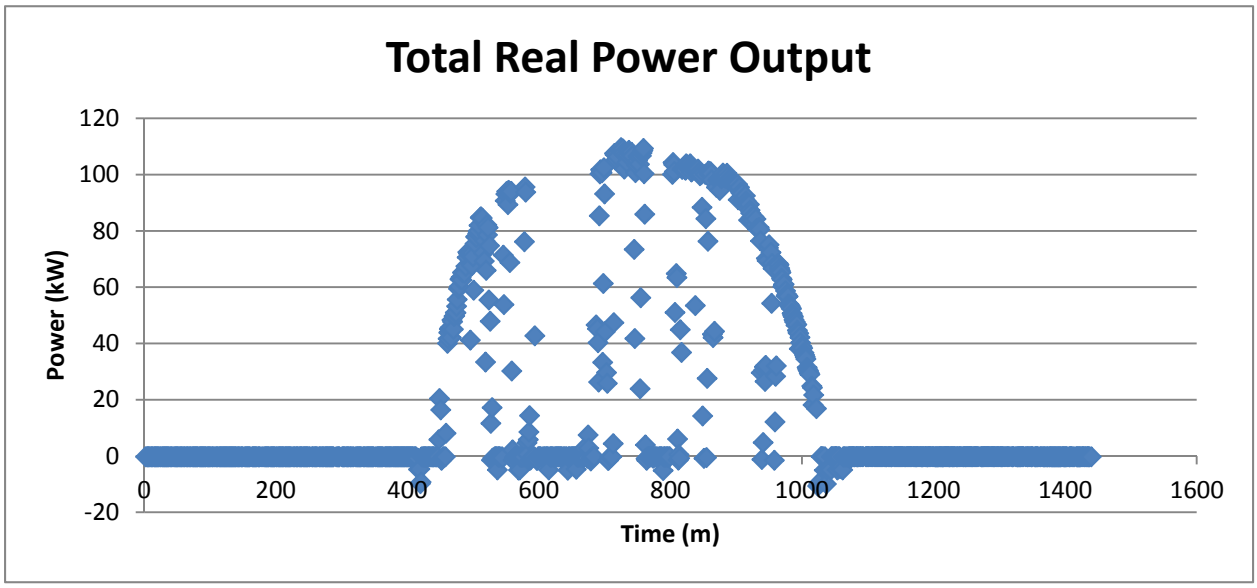

Figure 32. Typical Power Output Trend in the Presence of Intermittency Associated with Cloud Passage.

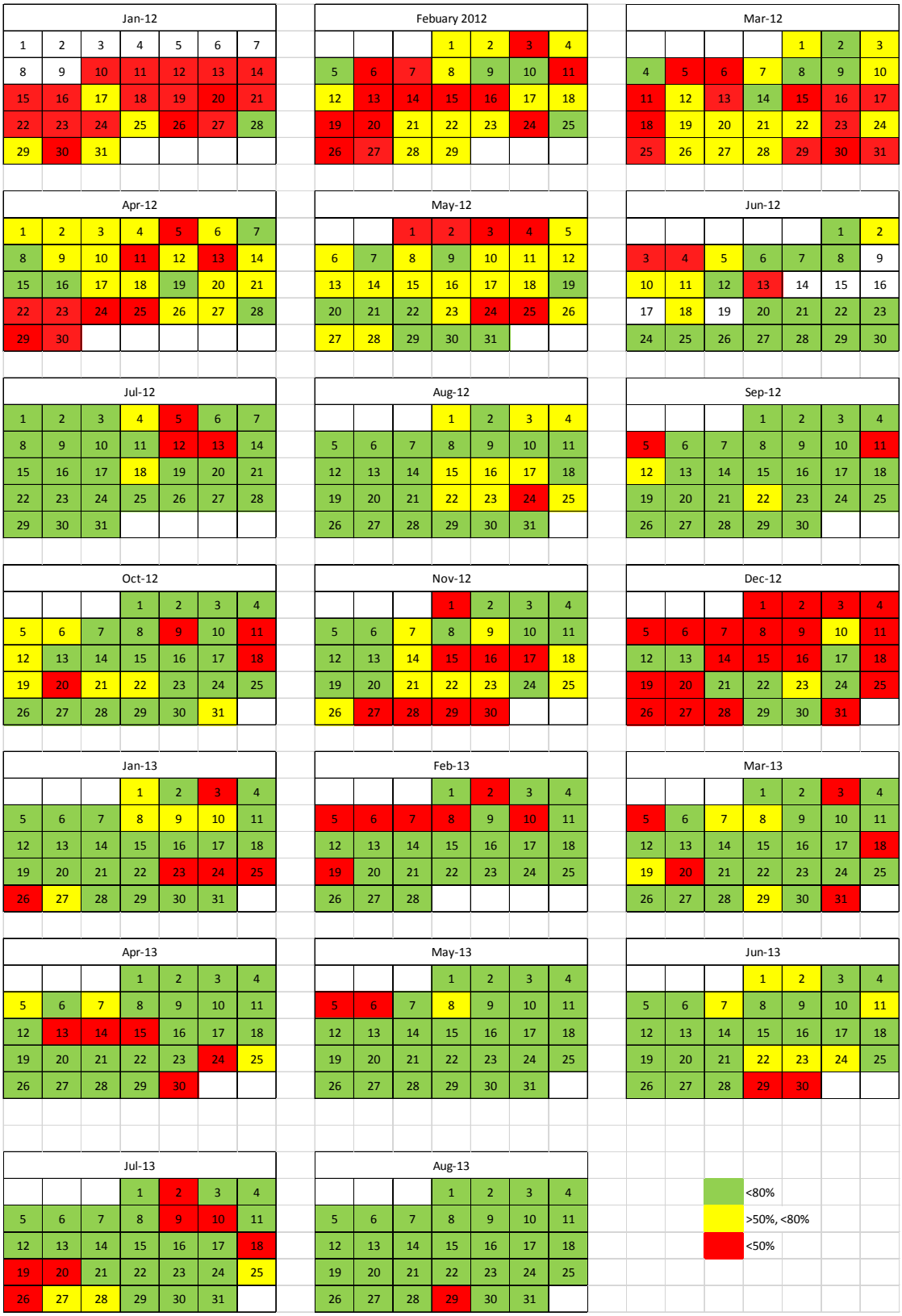

Figure 33. Impact of Intermittency on Energy Generation.

Measured CPV power generation profiles from both clear and cloudy days are inputted into the load flow model to investigate the effects on intermittent power injection on local line voltages. In Figure 34, baseline and 2.0x baseline intermittent power profile simulations are run. Results show that due to voltage support from the UCI sub-circuit feeders, sudden changes in local power production do not result in excessive low voltage dips or flicker. The most severe changes occur at the inverter terminals which serve no directly attached loads and the voltages at the ARC-MCC bus remain relatively unchanged.

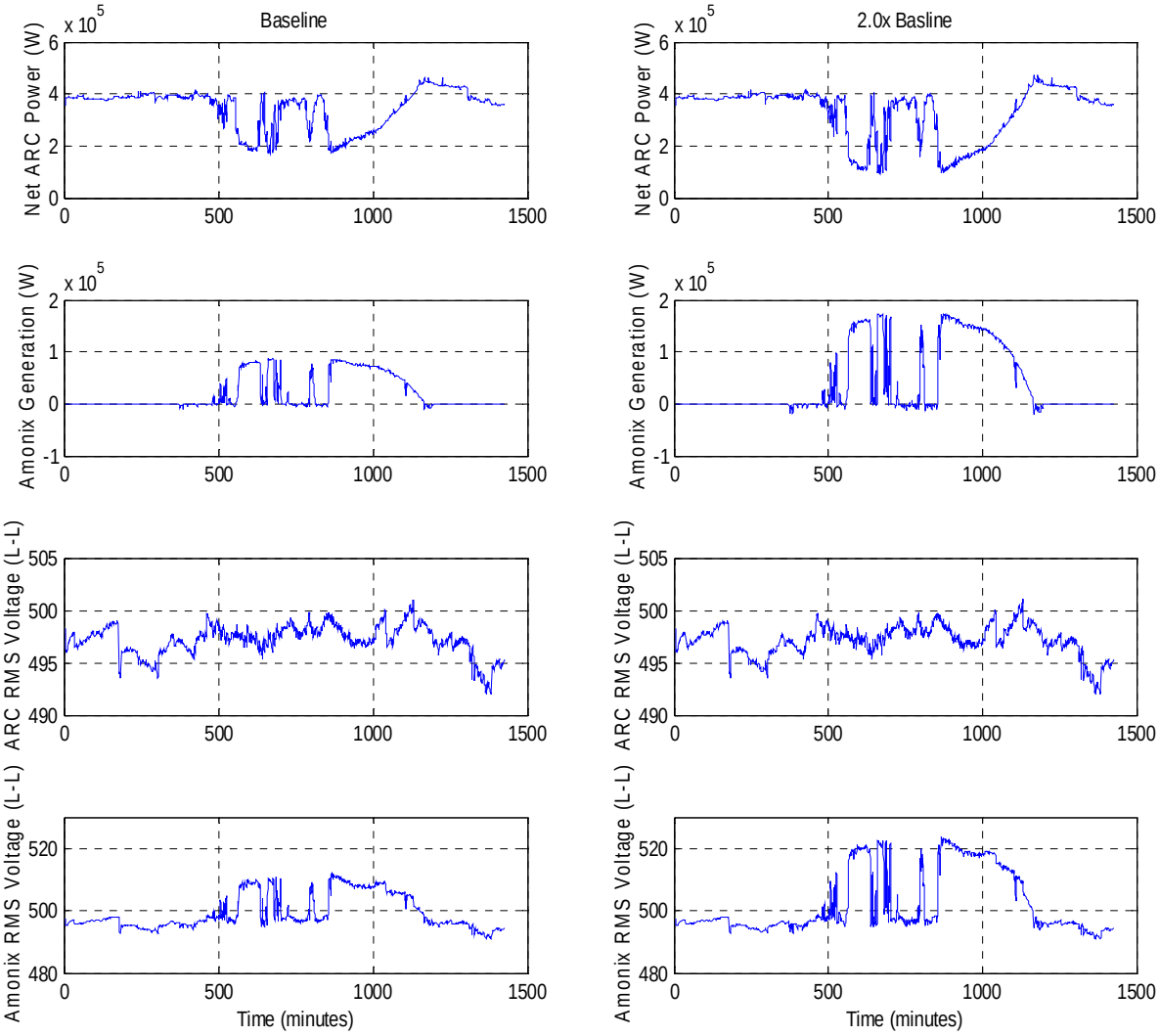

Figure 34. Simulation Results for a High Demand Day with Intermittent Generation. 7/5/2013.

3.2.2.3 Summary

- Excessively high terminal voltages were noted. Possible remedies include increasing the CPV-7700 to ARC-MCC conductor size, operating at a lagging power factor, or utilizing a dedicated step-up transformer to directly couple to the 12.47kV feeder.
-

3.2.3 Impact of High Penetrations of CPV on UCI Circuits

ETAP simulations were conducted to simulate varying penetrations of CPV on the UCI microgrid circuits. This is achieved using the ETAP load flow model with the historical power profiles for the existing Amonix installation scaled to simulate the installation of additional Amonix CPV-7700 systems. Conductor diameters were scaled appropriately to accommodate the increased generation. Both inverter to ARC-MCC line losses and inverter losses were scaled linearly to generation increase. In addition to the amount of CPV generation, the locations of the CPV 7700 systems were also altered in simulations to investigate the effects of relocating the installation sites to the beginning, middle, and end of the UC 1-10 sub circuits. Line losses and voltage effects were considered.

3.2.3.1 Increased CPV Penetration

ETAP simulations show that a 120kW (2x baseline) in situ increase in CPV generation may be tolerated at the original ARC site before inverter shutdown voltage limits are reached. Increasing the diameter of the inverter to ARC-MCC conductor, operating at a non-unity power factor, or relocating the installation closer to feeder circuits may lower terminal voltages. ANSI voltage tolerance band voltages are defined at -13%/+6% of nominal line voltage (398V to 508.8V for 480V L-L) and the system currently operates at +10.4%. The 350MCM conductor is rated for an ampacity of 380A and allows for approximately a 3.3x baseline generation increase before current limits are reached. Power injection at the 480V level up to these limits produces negligible voltage effects at the ARC-MCC in Figure 35. The injection of higher (up to 10x baseline) power directly on the 12.47 kV bus upstream of the ARC MCC also produces negligible voltage effects as shown in Figure 37. Figure 34 shows simulation results for relatively high ARC load coupled with intermittent PV generation. The ARC-MCC voltage profile tracks substation voltage, while the Amonix terminal voltage is dependent on real power injection. PV intermittency results in negligible effects beyond the ARC-MCC bus. Increasing the Amonix – ARC conductor diameter or installing of separate conductors for additional CPV-7700 eliminates the inverter voltage rise issue. Due to the relatively high R/X ratios of the conductors of 1.617, ampacity limits are reached before voltage stability limits. Figure 35 show the voltage profiles at the ARC and Amonix inverter terminals with varying levels of solar generation. As seen in the plots, the ARC-MCC voltage is negligibly influenced by power injection due to the presence of a large ARC load and a relatively stiff connection to the UCI substation. The high impedance of the cable connecting the inverters to the ARC-MCC cause a large voltage rise at the point of power injection. Figure 36 shows the line voltage at the reverse power flow limit (approximately 3.3x baseline generation). At this level, all produced power is immediately consumed by the ARC loads at peak demand. Line voltages at the ARC remain largely unchanged.

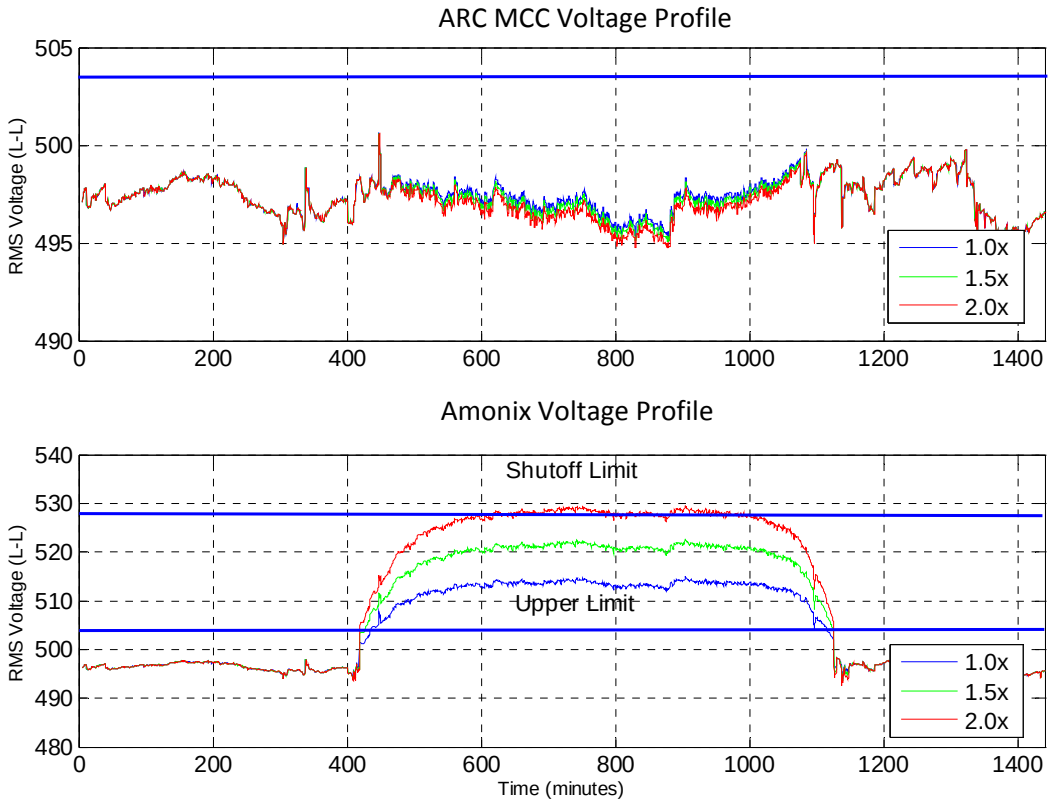

Figure 35. ARC and Amonix Simulated Voltage Profiles. 1.0x to 2.0x of Baseline Generation. 8/28/2013.

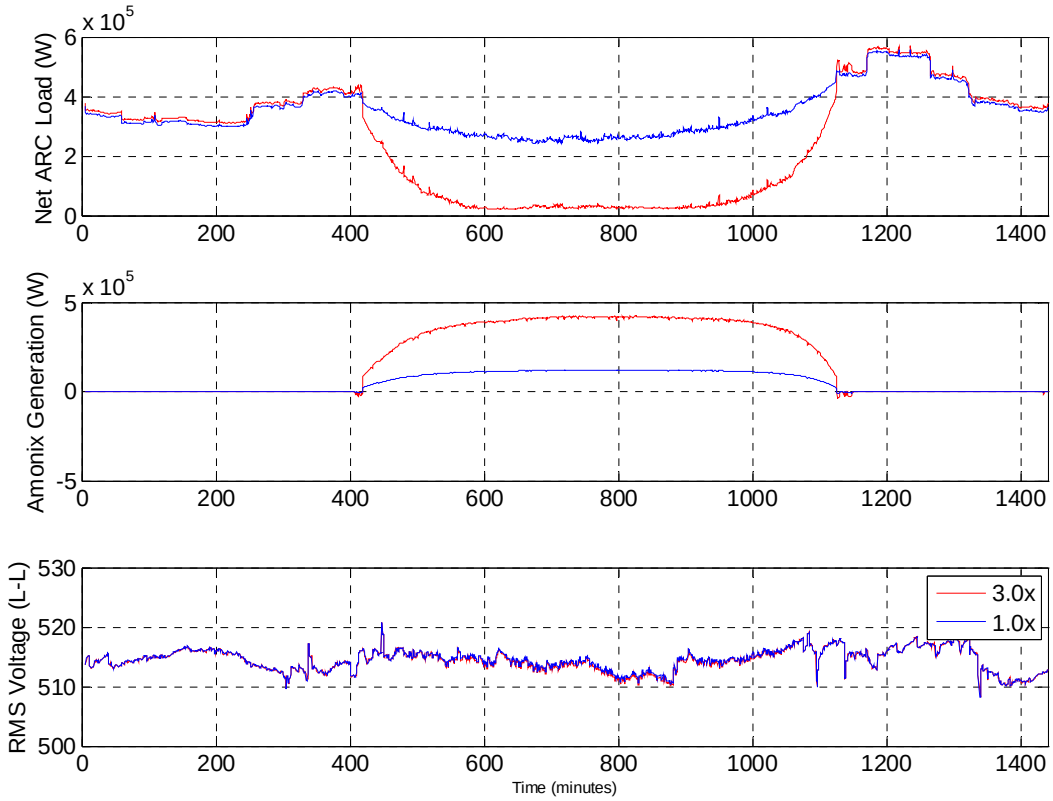

Figure 36. ARC MCC Reverse Power Flow Limit.

Power injection directly at the 12kV distribution line via a step-up transformer as opposed to local 480V buses yields considerably lower line voltage impacts, especially at high penetrations (>20x baseline) due to the direct connection to the feeder circuits. Simulation results indicate that at a 10x baseline generation increase (from 120kW to 1.2MW), the total change in line voltage is less than 0.54%. In these simulations, a CPV model element was introduced at the 12kV UCI-9 feeder circuit via the same 2MW transformer that services the ARC loads. Figure 37 shows the voltage impact at the transformer secondary with varying levels of CPV penetration.

As further increases in CPV capacity with the currently installed 1100' conductor would yield unacceptable inverter voltages, in all subsequent studies the distance from the CPV installation to the nearest bus has been reduced to 10' and the peak campus-wide operating voltage has been renormalized to 1 Vp.u. (480V L-L).

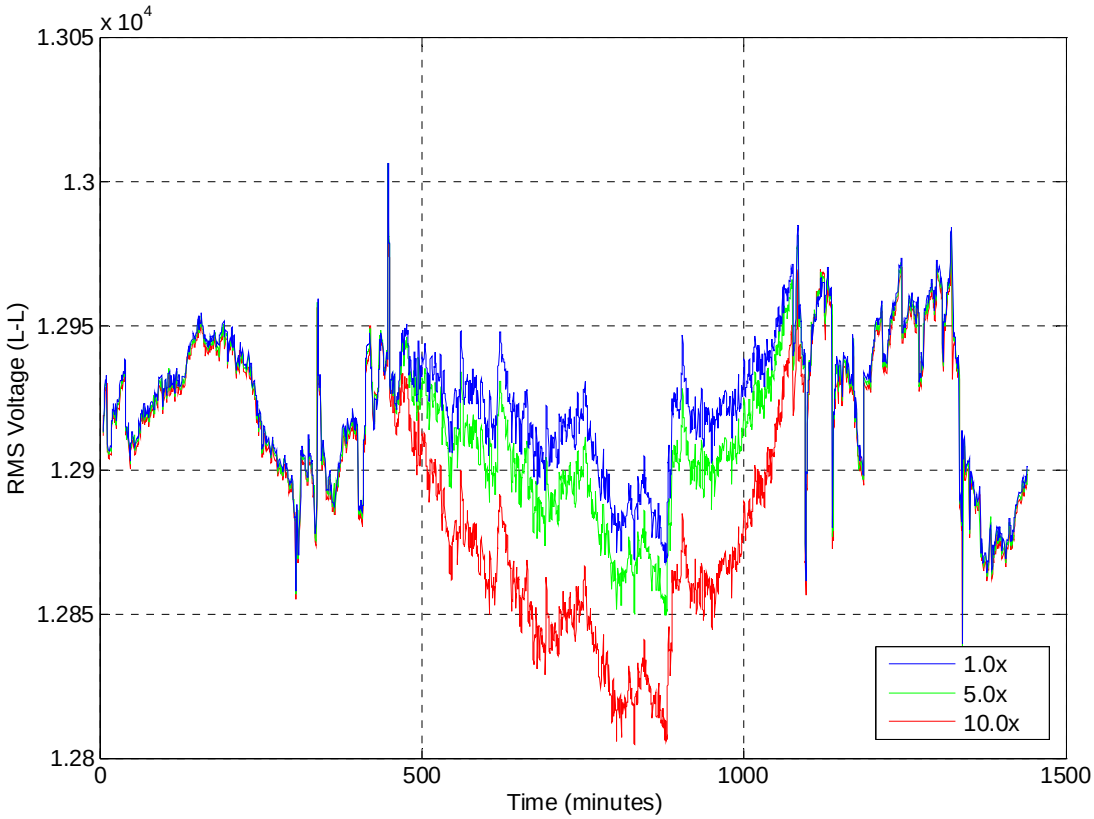

Figure 37. Direct 12kV Power Injection Voltage Profile Effects.

3.2.3.2 CPV Installation Location

In the UCI microgrid model, the installation location of the Amonix CPV-7700 systems was moved in simulation from the baseline (at the ARC) to the beginning (near substation), middle (nearest bus to the geographic middle), and end (according to electrical impedance) of the each of the subcircuits to evaluate the optimal location for future installations in terms of efficiency and voltage profile impact. Historical data from the existing ARC Amonix installation and building load data were used to determine normal operating points for the load flow studies used in these simulations.

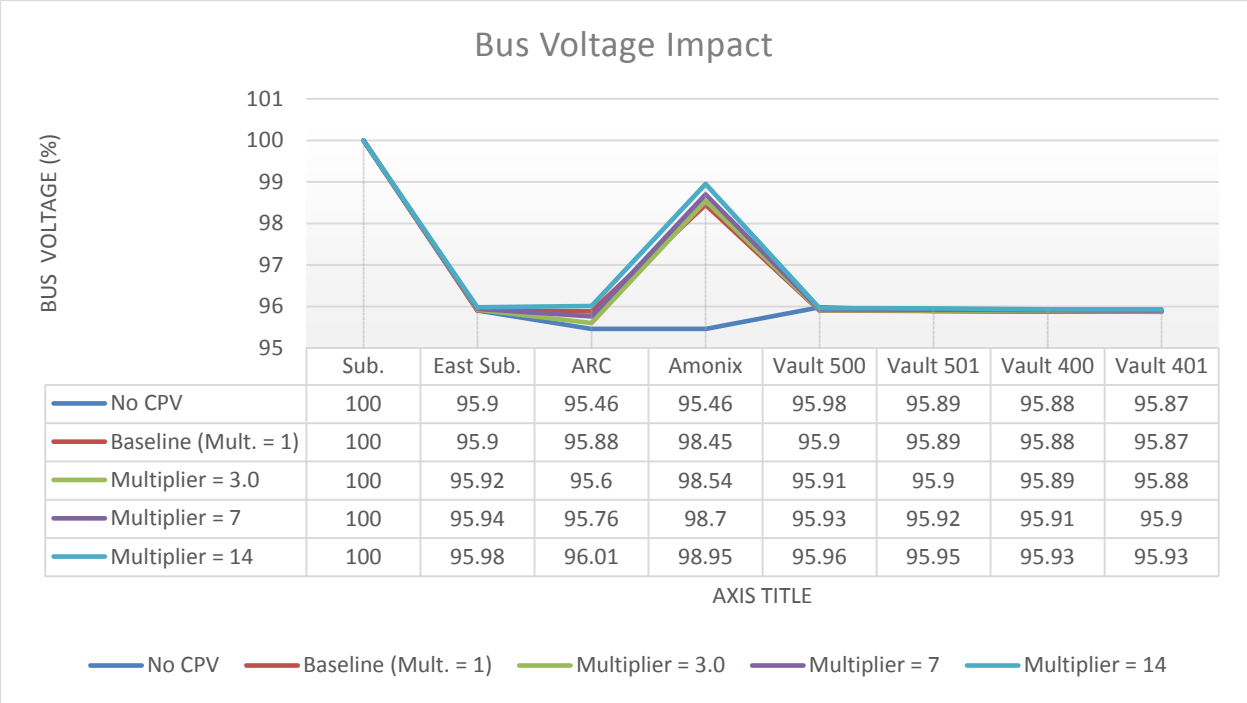

	Sub.	East Sub.	ARC	Amonix	Vault 500	Vault 501	Vault 400	Vault 401
No CPV	100	95.9	95.46	95.46	95.98	95.89	95.88	95.87
Baseline (Mult. = 1)	100	95.9	95.88	98.45	95.9	95.89	95.88	95.87
Multiplier = 3.0	100	95.92	95.6	98.54	95.91	95.9	95.89	95.88
Multiplier = 7	100	95.94	95.76	98.7	95.93	95.92	95.91	95.9
Multiplier = 14	100	95.98	96.01	98.95	95.96	95.95	95.93	95.93

Figure 38. Baseline Location Voltage Impact.

Figure 38 shows the impact of increasing CPV generation at the current ARC location. As seen in previous results, a high voltage rise is experienced at the Amonix bus, and a slight decrease is shown at the ARC-MCC and other busses along the circuit remain largely unaffected. These effects increase with generation capacity. Locally generated power is consumed primarily by the ARC and line losses related to delivering power from the UCI substation to the ARC-MCC are reduced when the Amonix system is producing power. This gain is slightly offset by the line losses incurred by sending power from the panels to the ARC-MCC and by inverter losses. When reverse power flow is established, transmission losses again begin to accumulate. Figure 39 and Figure 40 show the related line losses. The optimal operating point in terms of efficiency is achieved at approximately 450 kW, or the peak load of the ARC.

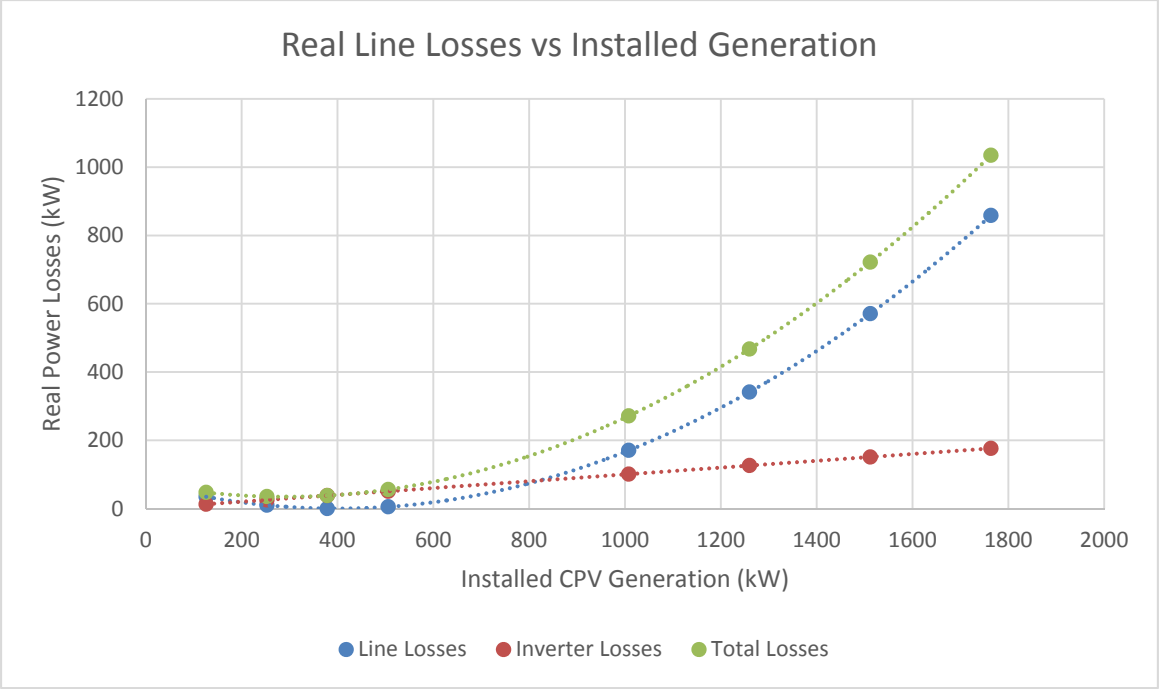

Figure 39. Baseline Installation Efficiency.

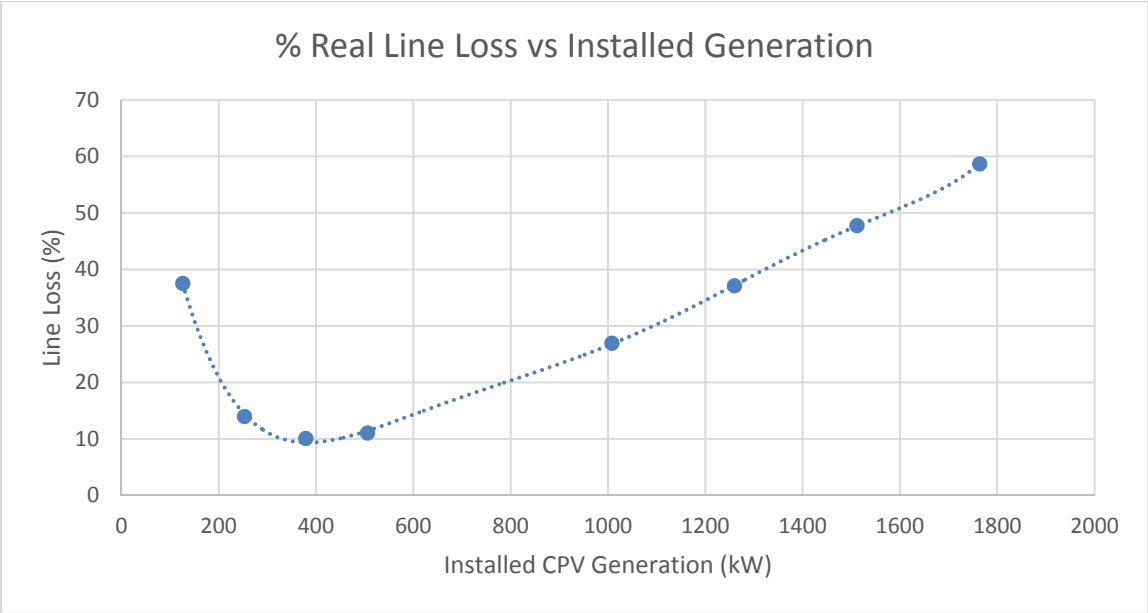

Figure 40. Baseline Percent Losses.

Moving the installation to the beginning of the UC-9 sub-circuit near the east substation results in a much stiffer connection the main substation. As a result of this, voltage effects due to power injection are greatly reduced. As there are no loads immediately at the east substation, any produced power may travel through the inverter-east substation conductor and then flow to

downstream loads, or travel the university substation and then to the grid. At this installation point, power generated is preferentially absorbed the by the UCI substation and reduces the net electric import, resulting in lowered line losses. Due to the large amount of voltage buffering provided by the east substation connection, a far greater amount of PV may be installed at this location. Figure 41 and Figure 42, Figure 43 show the voltage impact and line losses of this installation, respectively. Installation at this location results the greatest voltage stability, greatest overall system efficiency, and the widest allowable range of PV generation capacity.

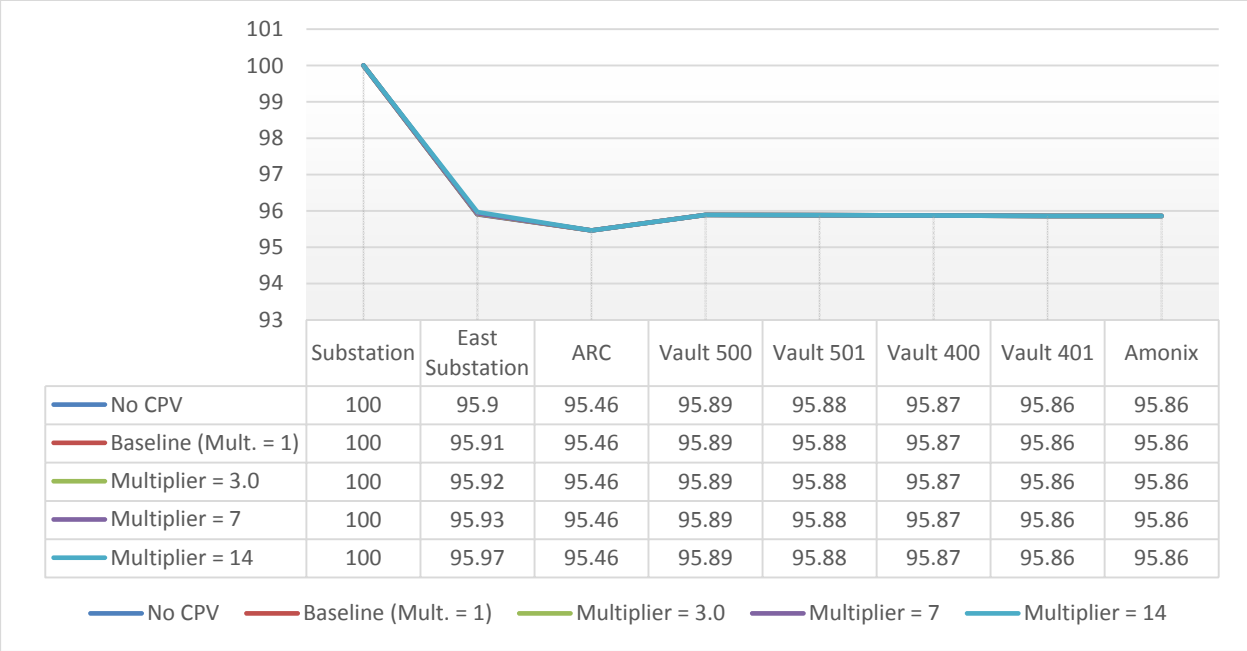

	Substation	East Substation	ARC	Vault 500	Vault 501	Vault 400	Vault 401	Amonix
No CPV	100	95.9	95.46	95.89	95.88	95.87	95.86	95.86
Baseline (Mult. = 1)	100	95.91	95.46	95.89	95.88	95.87	95.86	95.86
Multiplier = 3.0	100	95.92	95.46	95.89	95.88	95.87	95.86	95.86
Multiplier = 7	100	95.93	95.46	95.89	95.88	95.87	95.86	95.86
Multiplier = 14	100	95.97	95.46	95.89	95.88	95.87	95.86	95.86

Figure 41. Beginning Location Voltage Impact.

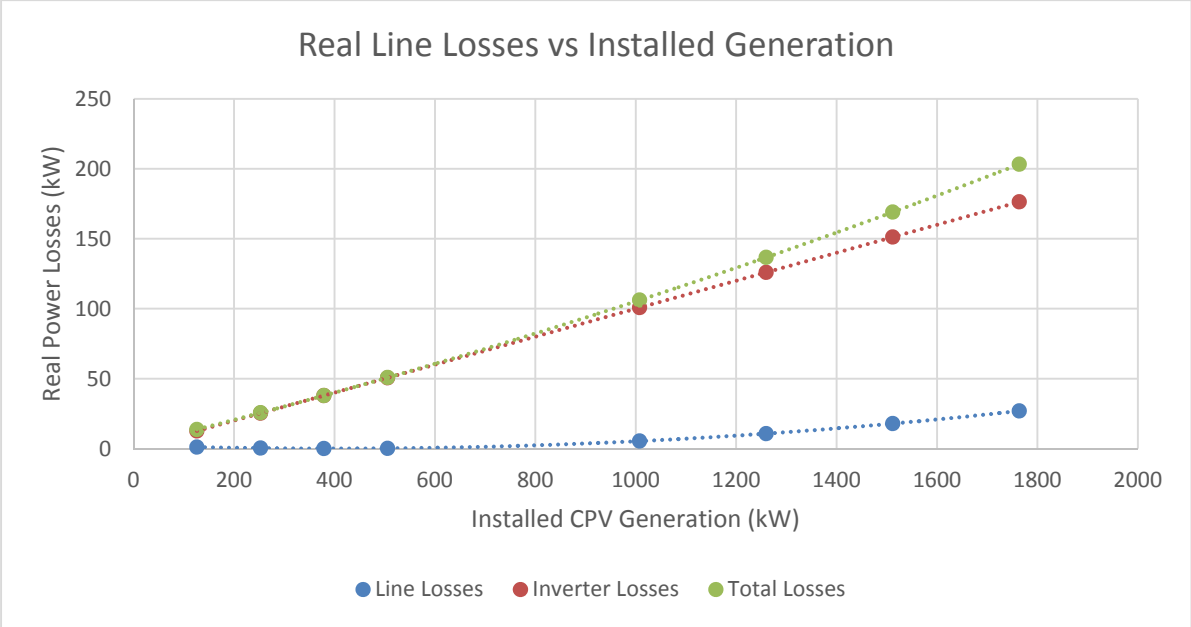

Figure 42. Beginning Location Real Power Loss.

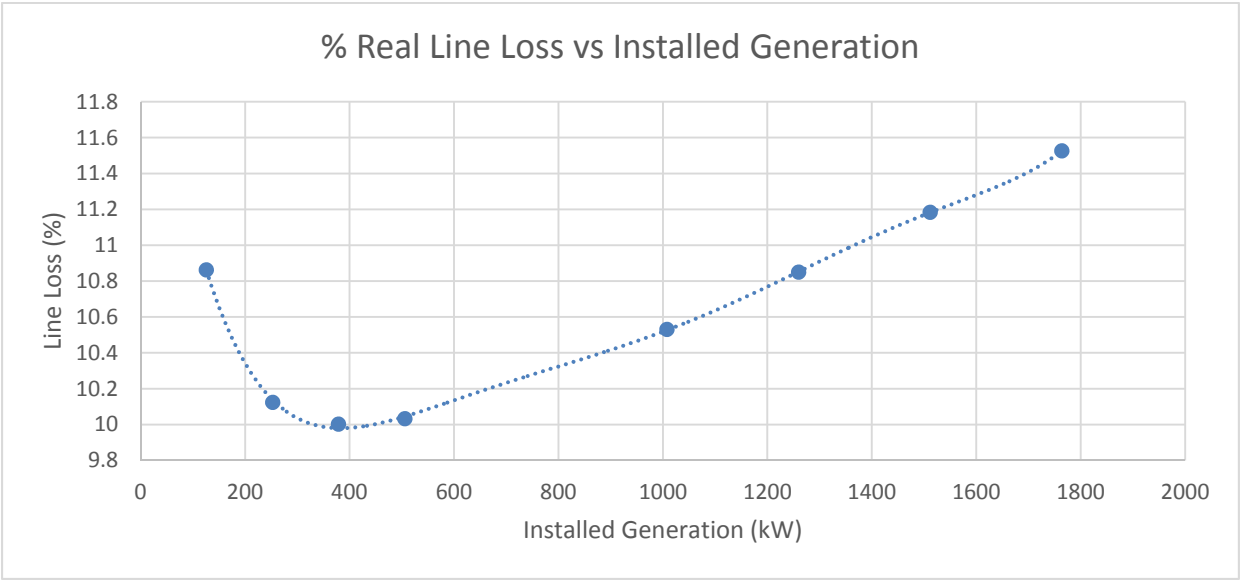

Figure 43. Beginning Location Percent Loss.

The vault 400 bus, located at the middle of the UC-9 circuit, serves the Engineering Gateway, Rockwell, and civil engineering building loads. An installation here results in a noticeable voltage increase at the inverter terminals followed by slight decreases in voltage at the adjacent busses. Line loss reductions gained by reducing the transmission of power from the substation to the vault 400 loads are counteracted by line losses incurred in sending power from the Amonix installation to the same bus. This may be partially reduced by moving the

installation closer to the bus. Figure 44 and Figure 45, Figure 46 show the middle installation voltage impact and line losses, respectively.

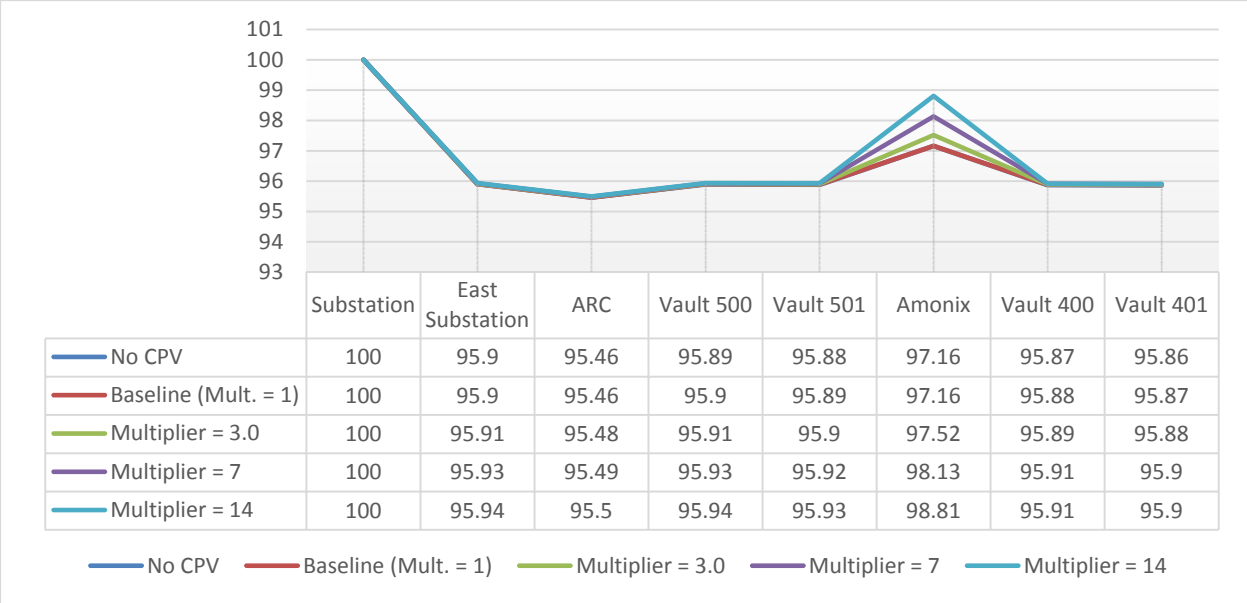

	Substation	East Substation	ARC	Vault 500	Vault 501	Amonix	Vault 400	Vault 401
No CPV	100	95.9	95.46	95.89	95.88	97.16	95.87	95.86
Baseline (Mult. = 1)	100	95.9	95.46	95.9	95.89	97.16	95.88	95.87
Multiplier = 3.0	100	95.91	95.48	95.91	95.9	97.52	95.89	95.88
Multiplier = 7	100	95.93	95.49	95.93	95.92	98.13	95.91	95.9
Multiplier = 14	100	95.94	95.5	95.94	95.93	98.81	95.91	95.9

Figure 44. Middle Location Voltage Impact.

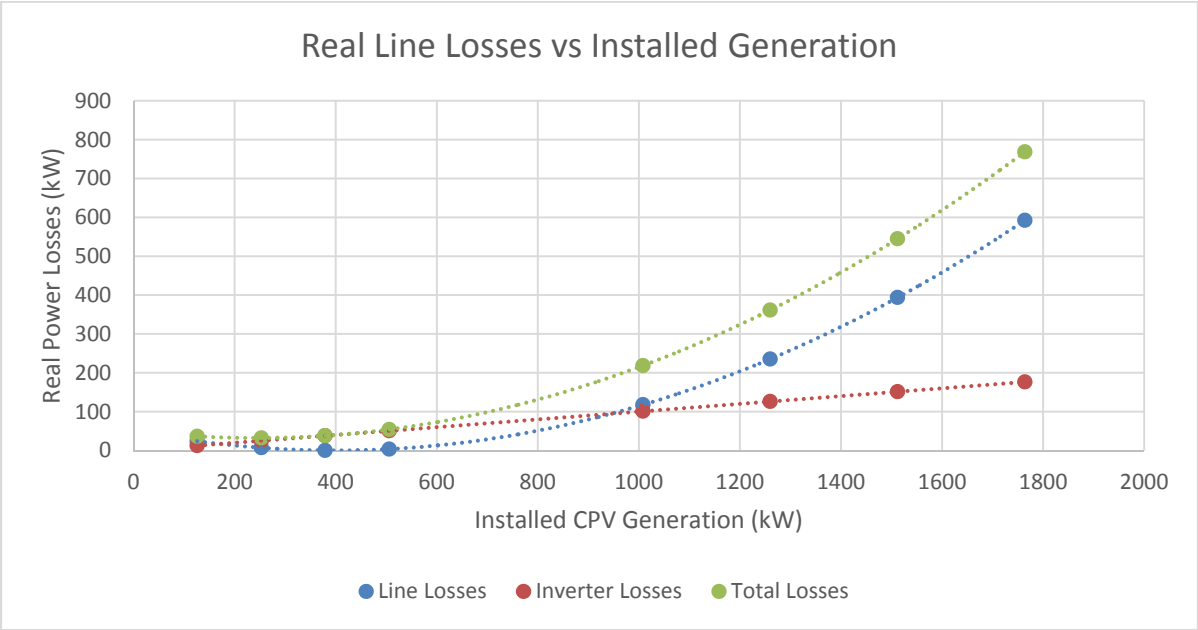

Figure 45. Middle Location Real Power Loss.

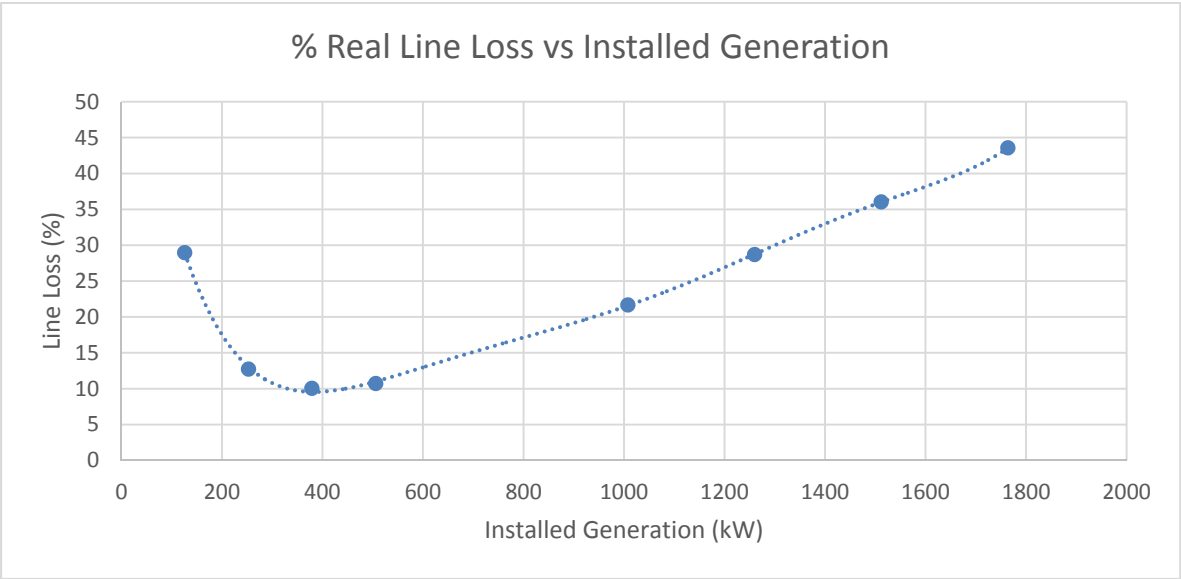

Figure 46. Middle Location Percent Loss.

Installation at the end of the circuit yields very similar results as the baseline installation. The ARC and the vault 401 bus are in similar in terms of distance from the UCI substation. Vault 401 serves the Engineering Tower and computer science building loads. At the end installation location the impedance between the substation and the site are the highest resulting in the highest incurred line power losses.

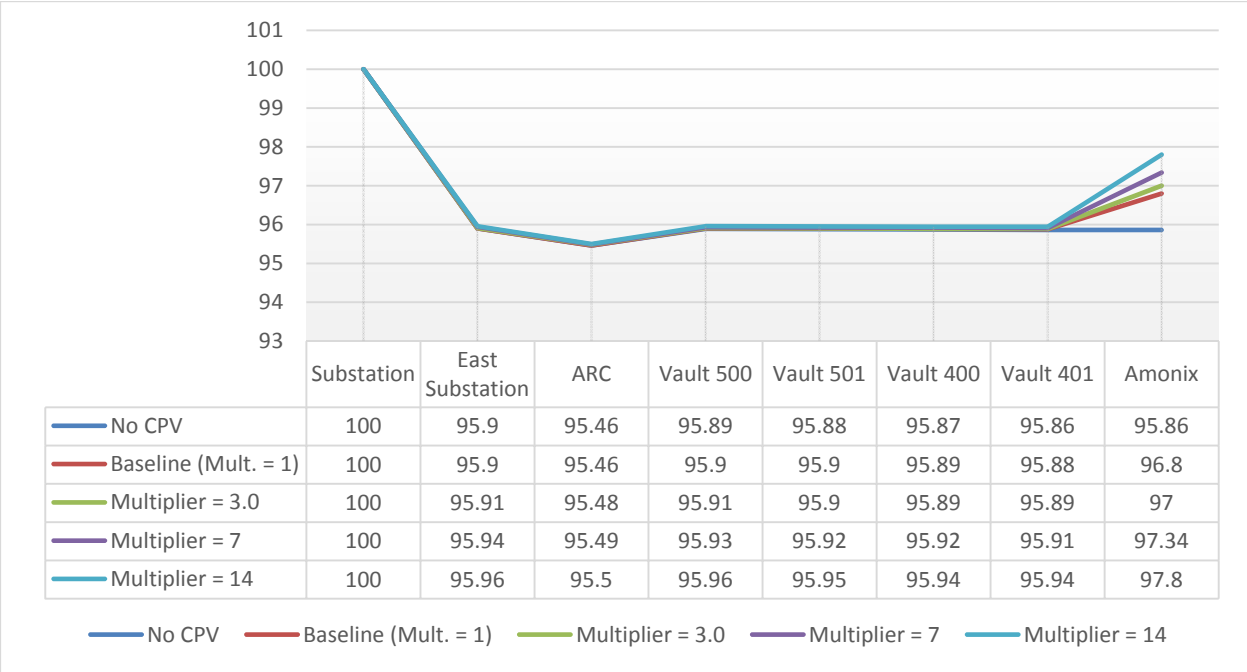

	Substation	East Substation	ARC	Vault 500	Vault 501	Vault 400	Vault 401	Amonix
No CPV	100	95.9	95.46	95.89	95.88	95.87	95.86	95.86
Baseline (Mult. = 1)	100	95.9	95.46	95.9	95.9	95.89	95.88	96.8
Multiplier = 3.0	100	95.91	95.48	95.91	95.9	95.89	95.89	97
Multiplier = 7	100	95.94	95.49	95.93	95.92	95.92	95.91	97.34
Multiplier = 14	100	95.96	95.5	95.96	95.95	95.94	95.94	97.8

Figure 47. End Location Voltage Impact.

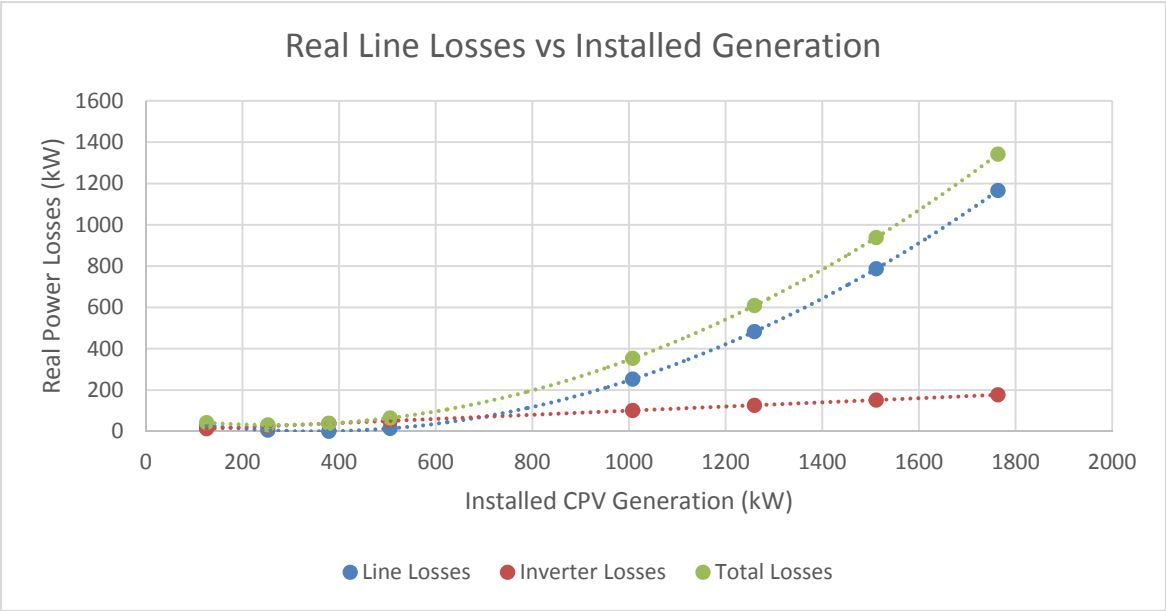

Figure 48. End Location Real Power Loss.

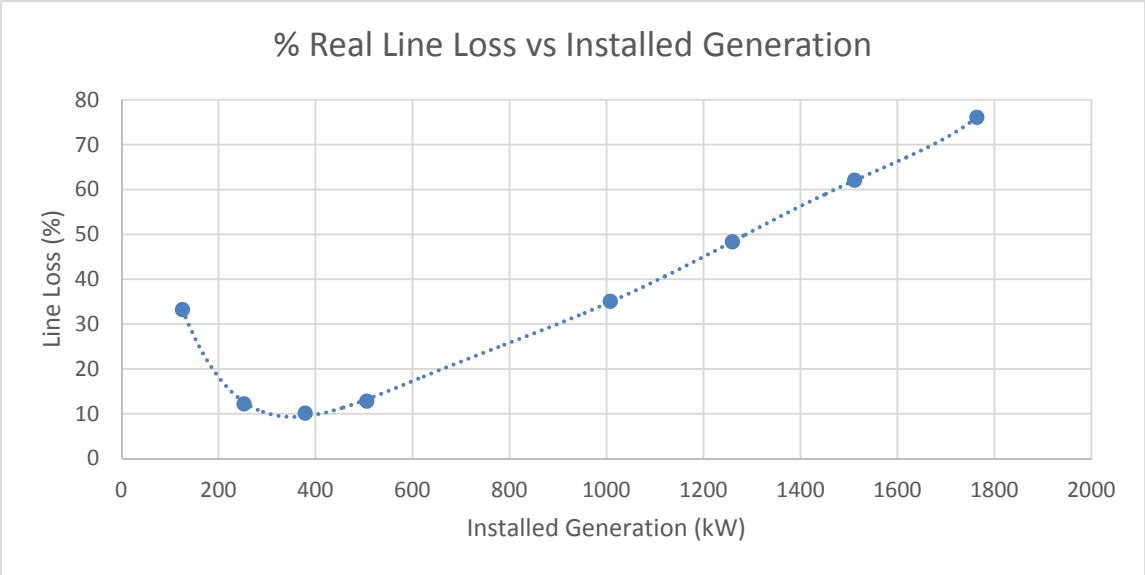

Figure 49. End Location Percent Loss.

In addition to increasing the generation capacity and moving the location of the installation along the UC-9 sub-circuit, the relocation of the Amonix CPV-7700 system to other sub-circuits was considered. In these studies, a CPV system was simulated at each of the UCI subcircuits with generation capacities of baseline (120kW), 5x (600kW) and 12x (1.4MW). The following chart summarizes the expected line voltage and efficiency implications of installing

additional CPV-7700 systems on other UCI subcircuits. In previous analysis, normal operating points were used as simulation variables. In these studies, historical data was used to determine worst-case operating scenarios to determine the absolute limits on CPV integration. In the voltage analysis case, the worst-case operating conditions occur when solar power is at a maximum and local loads are at a minimum. For efficiency studies, the worst case scenario was achieved by operating the furthest loads furthest from the solar installation at maximum load while maintaining light loading on nearby busses. The load values across all building loads were adjusted such that the summation of all loads equaled the historical total campus energy consumption. Simulations for the UC-7 circuit were not run due to lack of building energy data for that sub-circuit.

Table 4. UC1 – UC9 Worst Case Power Loss Analysis.

	UC-1	UC-2	UC-3	UC-4	UC-5	UC-6	UC-7	UC-8	UC-9	UC-10
LINE LENGTH (FT.)	3795	2170	1	40	1660	3770	X	3100	7835	90
% LOSS (BEGINNING) - BASELINE	12.15	11.23	10.00	10.02	10.9	12.13	X	11.75	14.44	10.05
% LOSS (MIDDLE) - BASELINE	20.76	16.15	10.00	10.11	14.70	20.69	X	18.9	32.12	10.25
% LOSS (END) - BASELINE	31.52	22.30	10.00	10.22	19.41	31.38	X	27.58	54.43	10.51
% LOSS (BEGINNING) – 5.0X BASELINE	10.21	10.12	10.00	10.00	10.09	10.21	X	10.17	10.45	10.00
% LOSS (MIDDLE) -5.0X BASELINE	11.09	10.62	10.00	10.01	10.48	11.09	X	10.89	12.26	10.02
% LOSS (END) - 5.0X BASELINE	12.19	11.25	10.00	10.02	10.69	12.18	X	11.79	14.53	10.05
% LOSS (BEGINNING) – 12.0X BASELINE	12.47	11.41	10.00	10.02	11.08	12.45	X	12.02	15.10	10.05
% LOSS (MIDDLE) -12.0X BASELINE	22.37	17.07	10.00	10.13	15.41	22.29	X	20.10	32.5	10.29
% LOSS (END) – 12.0X BASELINE	34.74	24.14	10.00	10.26	20.82	34.58	X	30.21	61.08	10.58

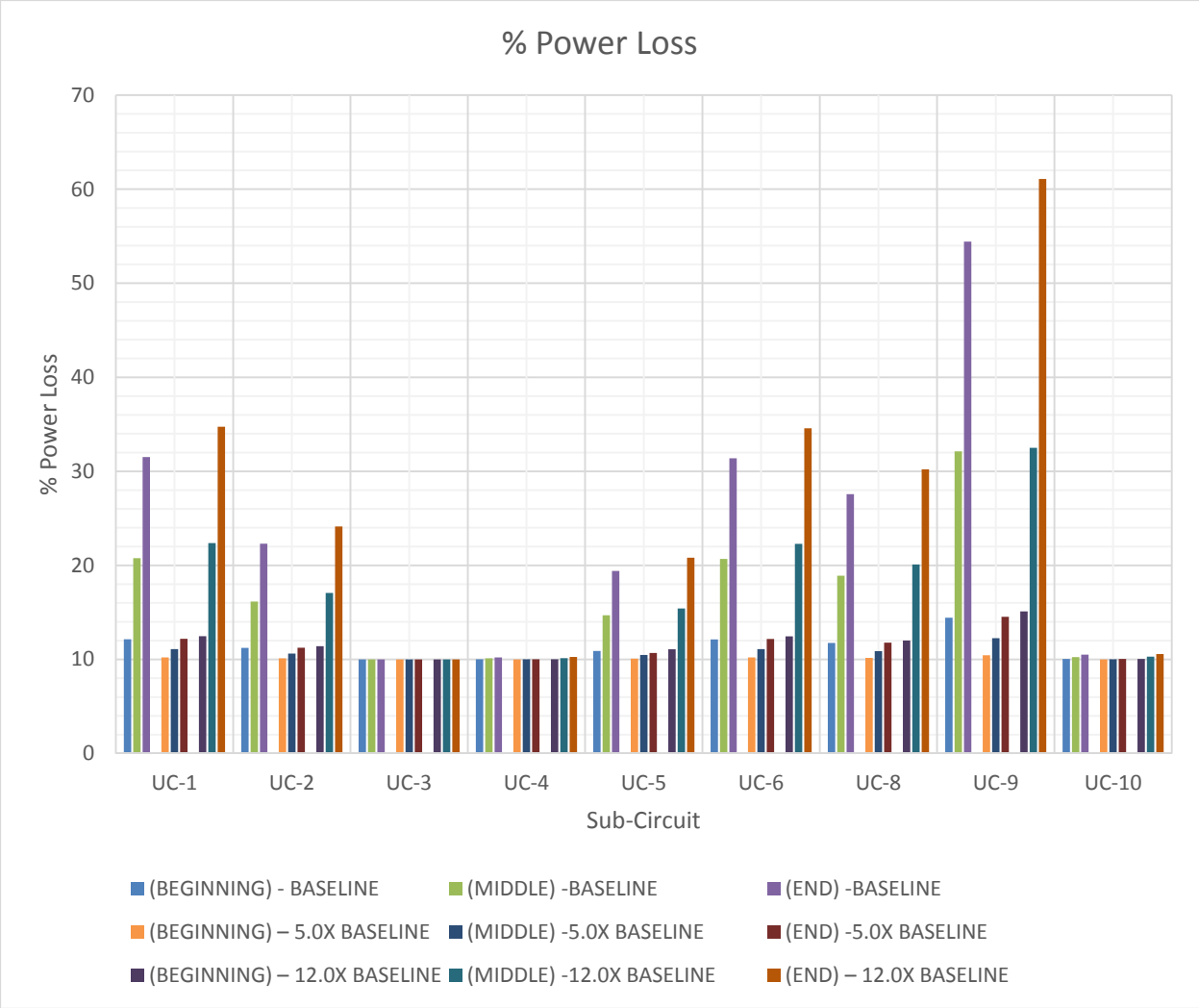

Figure 50. UC1 – UC9 Worst Case Power Loss Analysis.

It was noted that on all sub-circuits, limiting power generation capacity to that of local load demand yielded the lowest line losses. This is due to produced power being immediately consumed by nearby loads, avoiding transmission line losses. In the extreme case of the 12.0x baseline simulations nearly all sub-circuits with the exception of UC-3, 4, and 10 which are relatively short exhibit large (>20%) line losses in the worst case scenarios.

Table 5. UC1-UC9 Worst Case Voltage Rise Analysis

	UC-1	UC-2	UC-3	UC-4	UC-5	UC-6	UC-7	UC-8	UC-9	UC-10
LINE LENGTH (FT.)	3795	2170	1	40	1660	3770	X	3100	7835	90
% LOSS (BEGINNING) - BASELINE	0.68	0.39	0.000	0.007	0.29	0.68	X	0.55	1.41	0.01
% LOSS (MIDDLE) - BASELINE	3.42	1.95	0.000	0.036	1.49	3.40	X	2.79	7.06	0.08
% LOSS (END) - BASELINE	6.84	3.91	0.001	0.072	2.99	6.80	X	5.59	14.13	0.16
% LOSS (BEGINNING) – 5.0X BASELINE	3.42	1.95	0.000	0.036	1.49	3.40	X	2.79	7.06	0.08
% LOSS (MIDDLE) -5.0X BASELINE	17.11	9.78	0.004	0.108	7.48	17.00	X	13.98	35.34	0.40
% LOSS (END) - 5.0X BASELINE	34.25	19.57	0.009	0.360	14.97	34.01	X	27.96	70.89	0.81
% LOSS (BEGINNING) – 12.0X BASELINE	8.21	4.69	0.002	0.086	3.59	8.16	X	6.71	16.96	0.19
% LOSS (MIDDLE) -12.0X BASELINE	41.82	23.49	0.010	0.433	17.97	40.81	X	33.55	84.81	0.97
% LOSS (BEGINNING) – 12.0X BASELINE	82.16	46.98	0.021	0.866	35.94	81.62	X	67.11	X	1.94

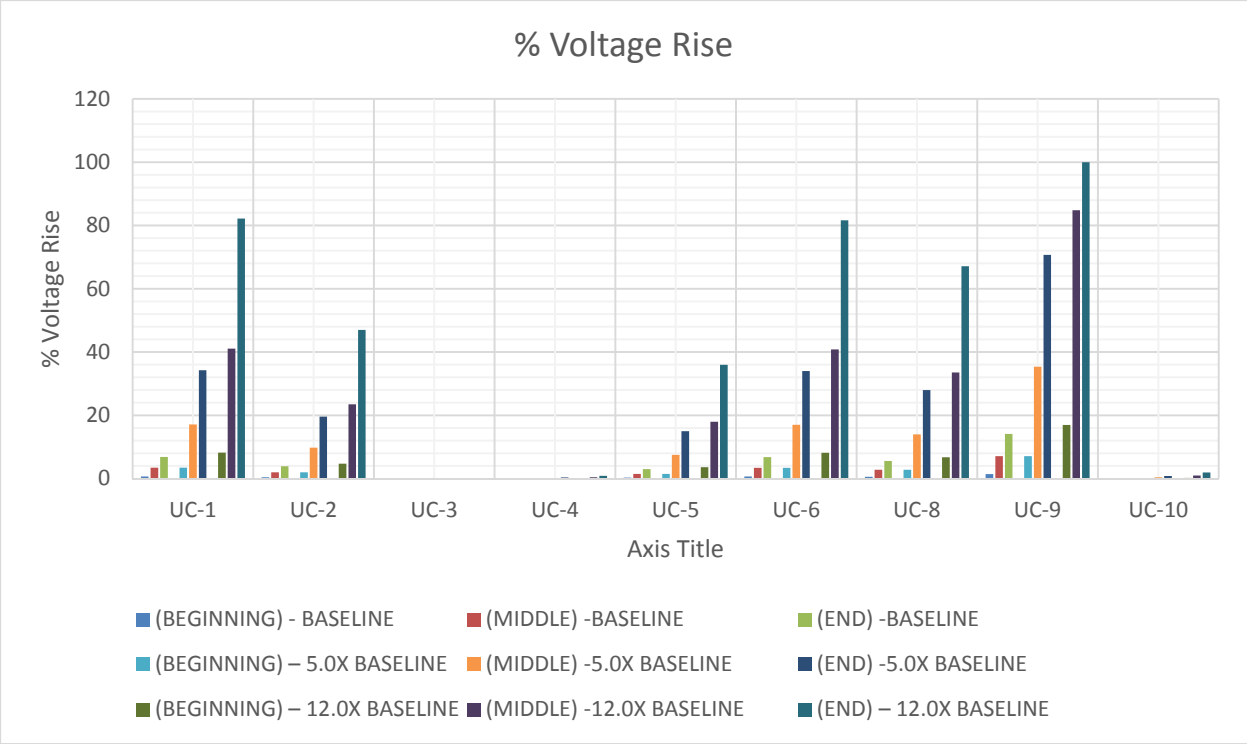

Figure 51. UC1-UC9 Worst Case Voltage Rise Analysis

Injecting power at unity power factor results in a voltage rise at the point of common coupling. In several cases on the UCI circuit, this voltage may be excessive. For circuits that are relatively distant from the substation, this proves to be an issue. Sub-circuits UC-1, 2, 5, 6, 8, and 9 are unable to support any CPV above approximately 360kW at any individual location at the 480V level without exceeding ANSI voltage tolerance limits while operating at unity power factor. Installing larger than this amount allocated at several locations throughout the sub-circuit or installing at the 12.47kV level would reduce overvoltage effects.

3.2.3.3 Summary

- The ARC net reverse power flow is achieved at a 3.34x baseline generation increase.
- Installation near the UCI substation results in the greatest voltage stability and minimizes line losses.
- From an efficiency standpoint, it is recommended for all sub-circuits to install CPV up to amount equal to the peak demand of the immediate locations' electrical demand. Further CPV capacity at the location results in increased line losses.
- UC-3, 4, and 10 are ideal candidates for large installations at the 480V level due to their proximity to the UCI substation.

3.3 Experimental Platform Development

The development of a test platform allows for experiments and proof-of-concept testing; the Connectivity Lab at the Advanced Power and Energy Program is a platform that allows for the real world microgrid experimentation. The lab consists of three identical nodes, each containing a 3.6kVA load, 5kW photovoltaic simulator, and an inverter to represent a typical residential installation. The connections between nodes are designed to be reconfigurable. One 12kVA AC source acts as a grid simulator. All devices are fully programmable and computer controlled, allowing for the simulation of transients, power distortions, and faults. Field data can be imported from devices such solar panels, fuel cells, and smart meters and replayed as well. The lab is designed to be modular and easily upgradable. It is anticipated that as the lab grows, additional devices will be added to augment the capabilities of the lab. Such devices may include fuel cells, battery storage, DG turbine generators, and automated demand response devices. Figure 52 and Figure 53 show the components of the Connectivity Lab.

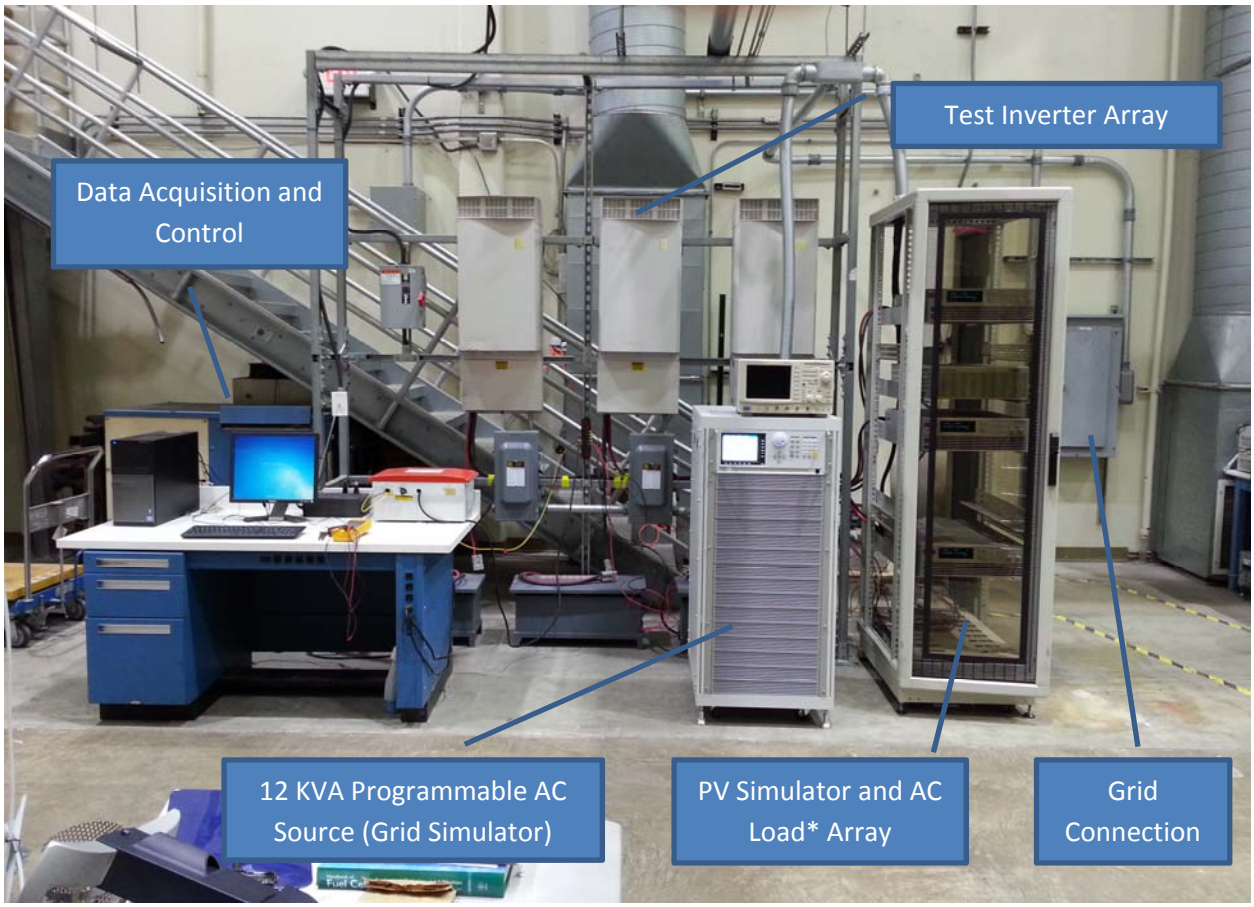

Figure 52. The UCI Connectivity Lab (*AC loads not shown)

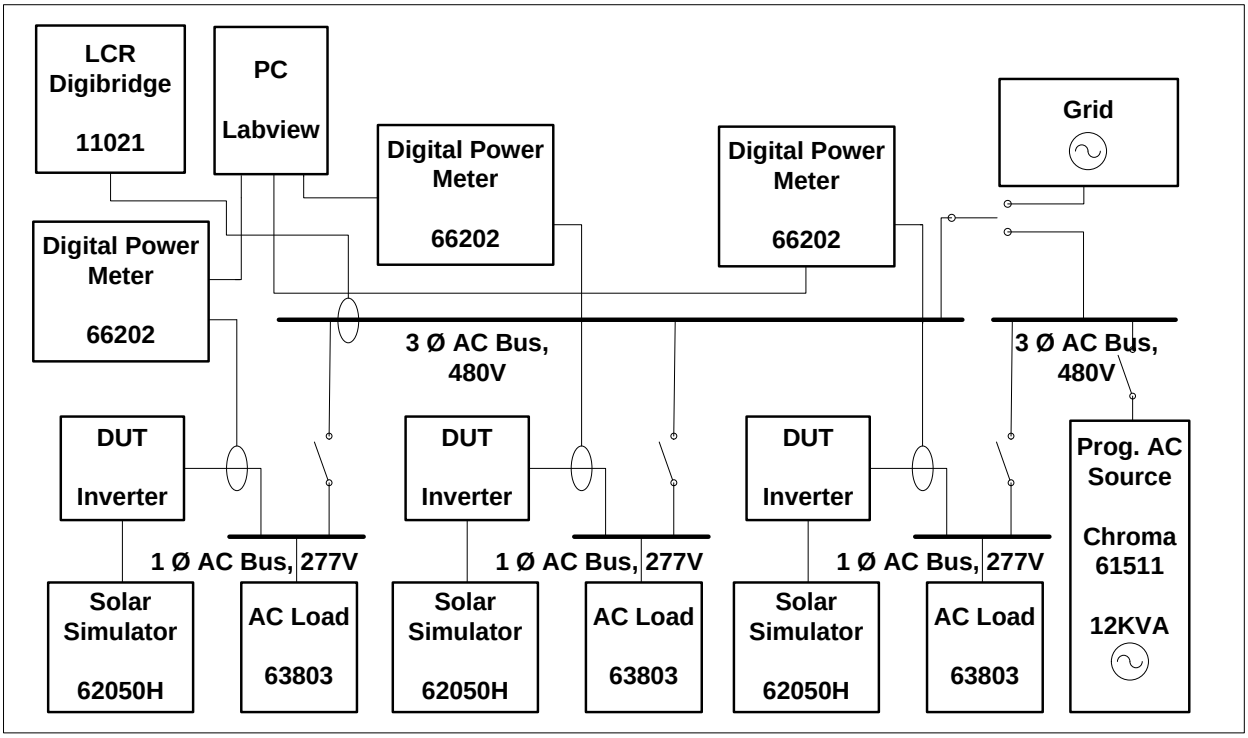

Figure 53. Connectivity Lab Component Diagram

To validate simulations, 1 sample per minute measurements from the Amonix installation were used to create a power generation trend which was recreated using the PV simulators and inverters. Similarly, the ARC load power trend was recreated using the programmable AC loads. To adjust the apparent grid impedance, the impedance emulation feature on the programmable AC source was used instead of passive impedance elements. Trend power values from original measurements were scaled down by a factor of 10 to accommodate the limitations of test equipment and the resulting voltage profiles were readjusted in post-processing of experimental results to reflect the original power levels. Field samples were recreated at a 5 minute granularity.

In the validation experiment, the AC source was configured as a grid emulating voltage source, the AC loads as dynamic loads, and the PV simulators as insolation following current sources. Figure 54 shows a comparison of inputted scaled Amonix inverter output field data vs. Connectivity lab inverter output measurements. A slight response delay was noticed due to the inverters attempting to track the field data command reference, and a decrease in transient response was noted.

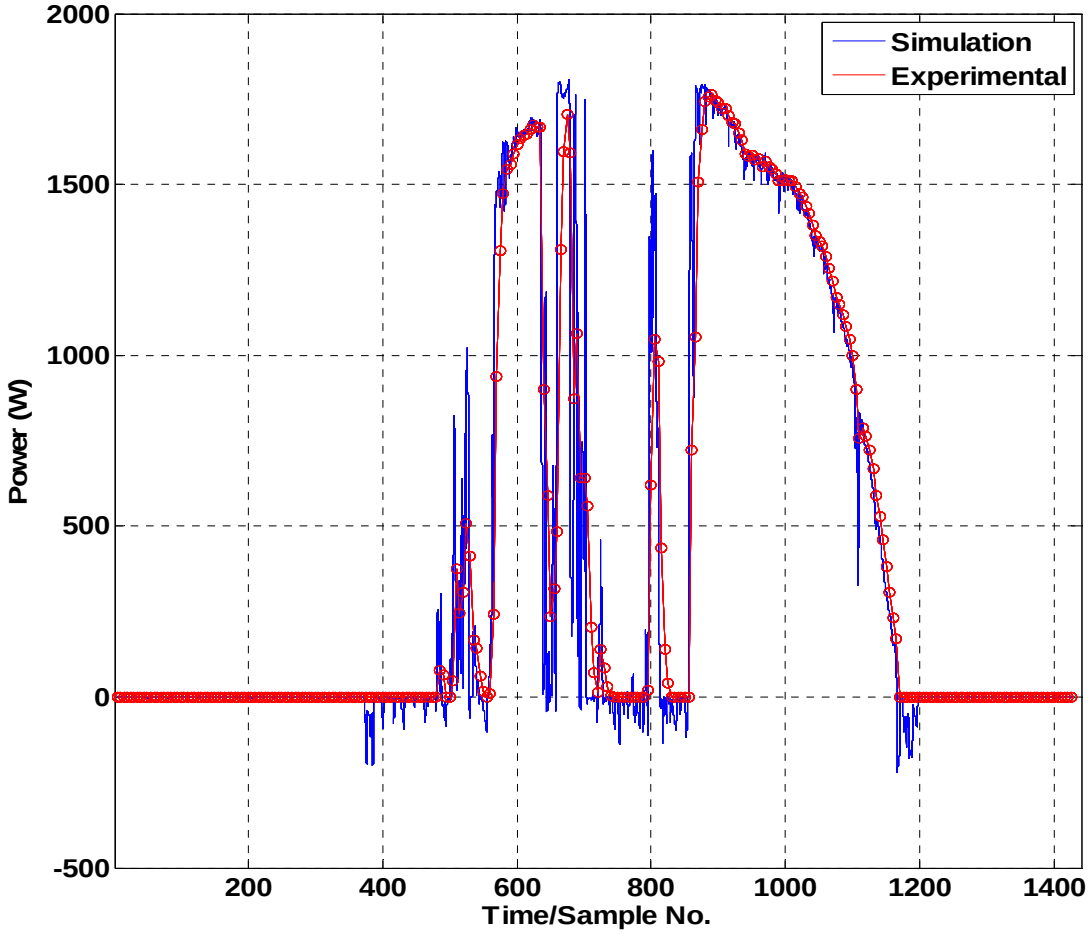

Figure 54. 7-5-2013 Dataset Simulation vs Experimental Results (Baseline)

As previously suggested, one possible remedy for the high line voltages observed at the UCI Amonix installation is to provide reactive power support to suppress voltage rise. The Solectria inverters may be equipped with a reactive power regulation component that allows the for variable power factor operation. The inverters are rated at combined apparent power capacity of 164 kVA of which only 120 kW of capacity is utilized. This leaves approximately 111.74 kVAR of reactive power capacity when operating at full real power output as shown in

Figure 55. Simulations conducted in both the ETAP and Simulink modeling environments have supported this claim and the Connectivity Lab was used to simulate the effects of reactive power injection in a scaled down scenario.

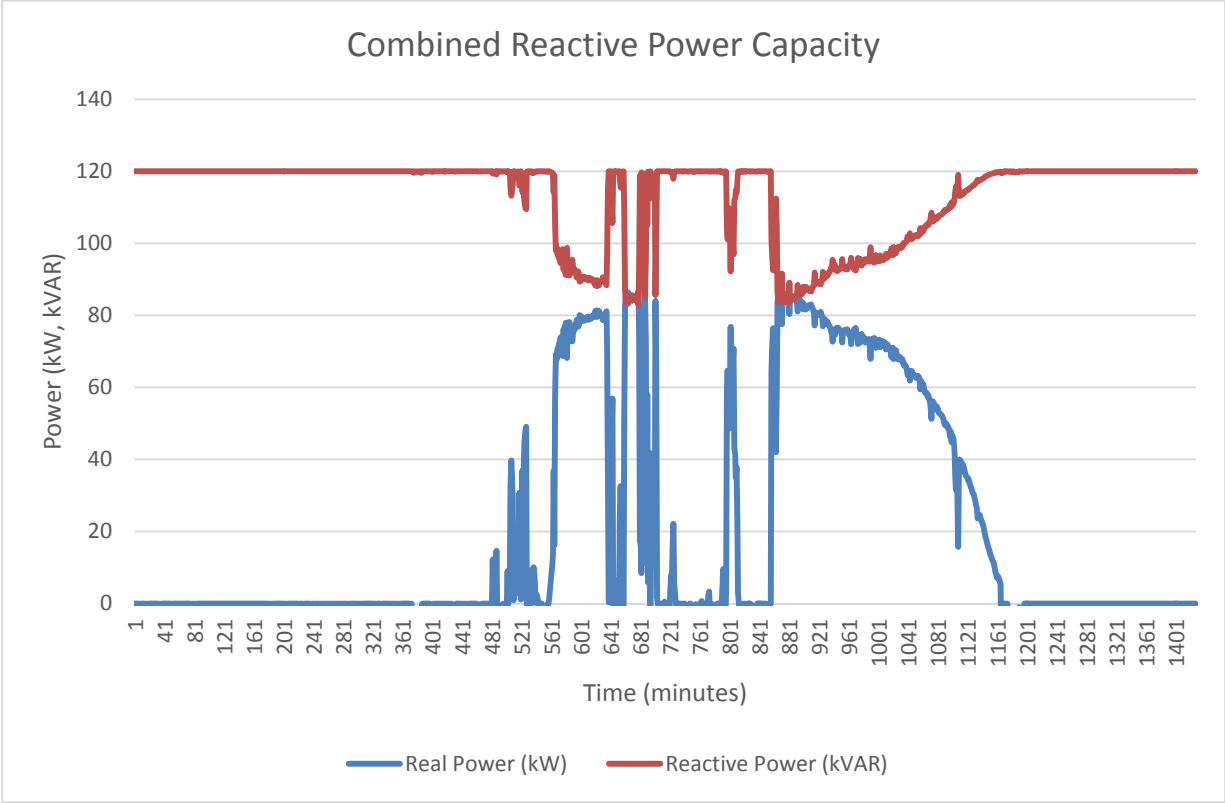

Figure 55. Reactive Power Generation Capacity vs Time.

An investigated strategy to alleviating the high voltage condition seen at the MCC bus involves utilizing spare inverter capacity to produce reactive power. The Connectivity Lab was used to validate reactive power voltage support simulations (the use of reactive power injection at a local node to regulate line voltages). In the following experiments, the Connectivity Lab was used to simulate varying levels of reactive power support provided by the Amonix installation. This is achieved by connecting the components of the laboratory to represent the conditions of the Amonix installation site and varying the power factor setpoint of the programmable AC loads. As direct control over inverter reactive power generation was not available, adjusting reactive power consumption of the directly attached AC load was done to emulate the same effects. The virtual impedance simulation feature on the AC source was also used to vary the impedance between the source and loads, to simulate the effect of varying the line impedance between the Amonix inverter terminals and the ARC-MCC. Due to the limitations of the Connectivity lab test components, power was scaled from 120 kW to 12kW and voltage scaled from 480V L-L to 277V L-L. All experiments were conducted on a single phase of a three phase 277V circuit.

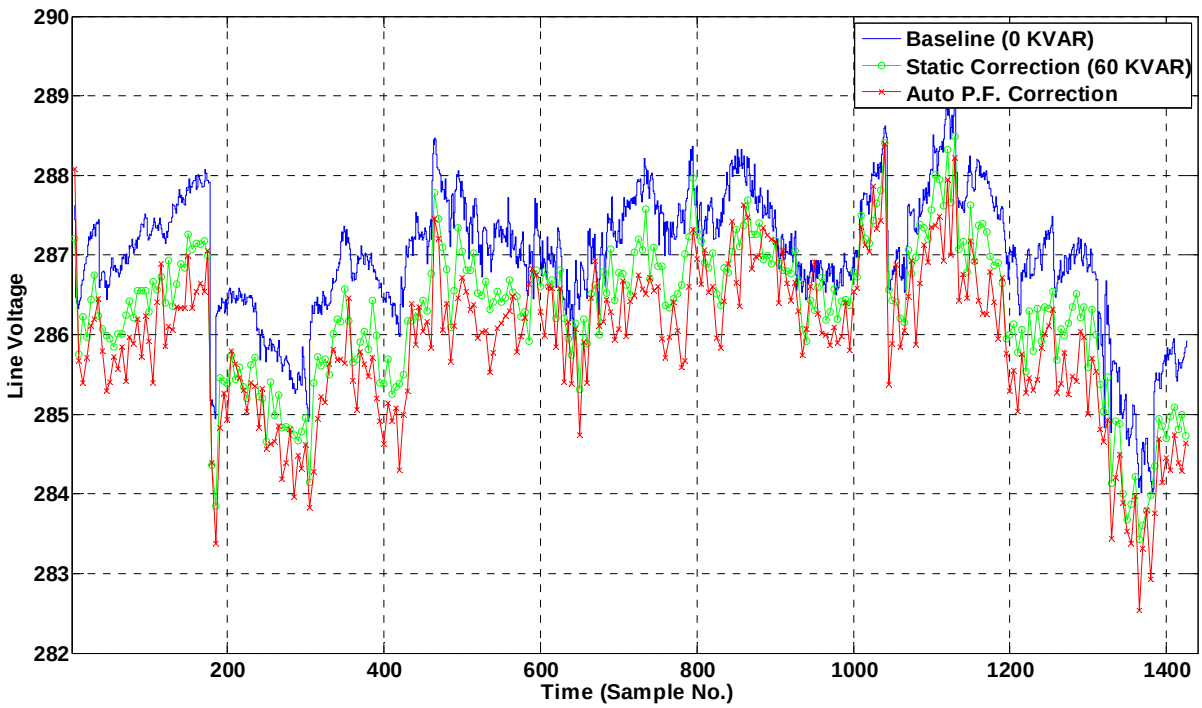

Figure 56. Reactive Power Support – Experimental Results.

Three reactive power support scenarios were experimentally simulated. The first scenario operates all system devices in unity power factor mode (0 KVAR). The second scenario operates the AC loads at (-Q = P, or P.F = -0.7). In the third case, all available spare generation capacity is allocated to reactive power generation. The controller consists of a reactive power set point adjuster that inputs a command variable according to:

$$Q_{setpoint} = \sqrt{(120kW)^2 - P^2}$$

It was observed that experimental results closely matched simulations with the exception of time periods of high output variability. This was likely caused to the lag effect of the maximum power point tracker mechanism within the inverters, which was not included in the simulation model. The maximum power point tracker requires a 5 – 30 second settling time to converge on the appropriate output power value. Reactive power injection at the local inverter node resulted in a voltage suppression at the ARC-MCC. While in simulations it was shown that the maximum voltage regulation is approximately 0.36 V.p.u. with the current line parameters higher inverter to feeder impedances would result in a greater voltage regulation band.

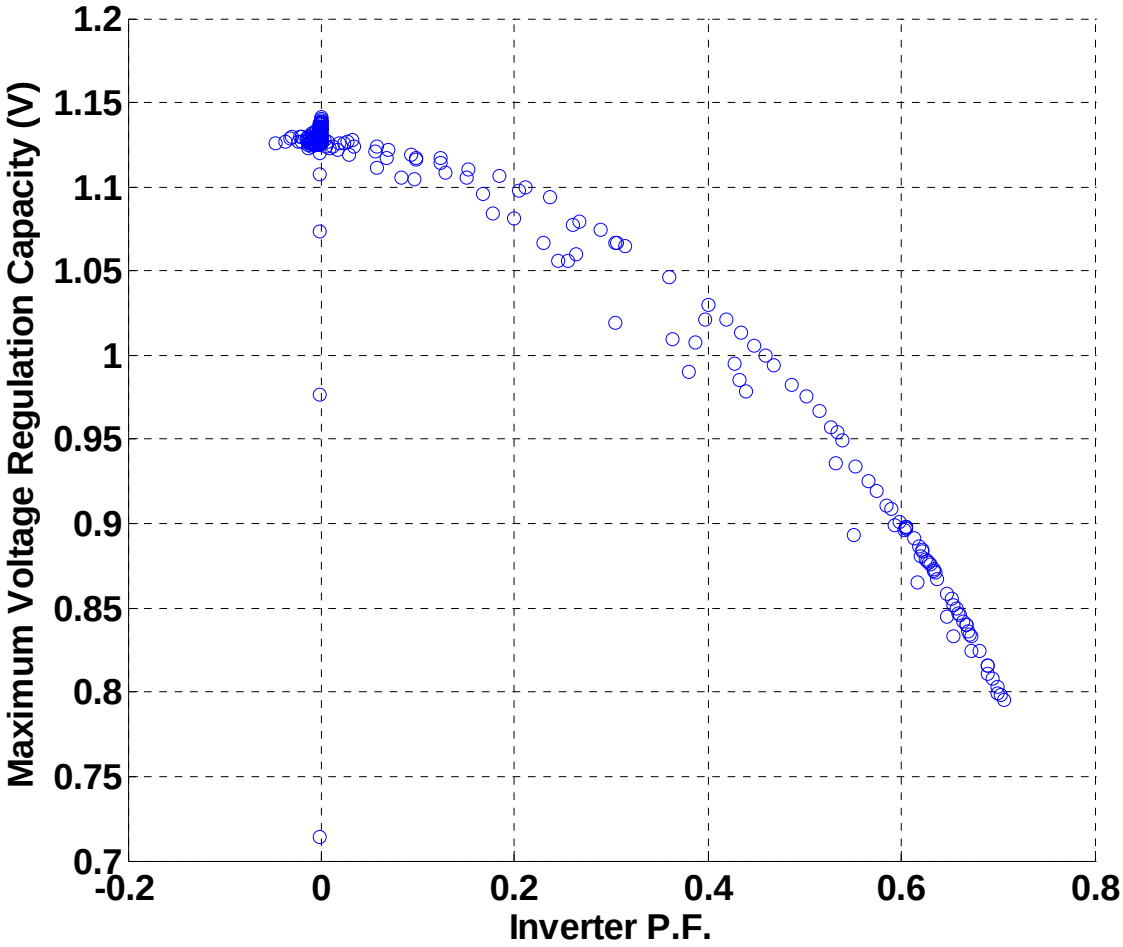

Figure 57. Reactive Power Voltage Support Limits.

4 Summary and Conclusions

This report is the second deliverable due under Subtask 2.3 and summarizes the operation of the campus electric system with regard to the installed campus CPV resources. The first report section discusses 1) the Amonix installation on the UC-9 circuit, 2) data collection, and 3) assesses CPV system performance. The second report section discusses the development of electric and CPV system models and how those models were used to evaluate the impacts of CPV systems on the UCI distribution system.

Two Amonix CPV 7700 system were installed at the eastern side of the University of California, Irvine campus at 33° 38' 23.29" N, 117° 49' 30.33" W. Both systems were connected to the UC-9 12kV feeder. Each system contains a 21 x 12 module CPV array mounted on a two-axis tracker and an 82kW Solectria 7700 PVI inverter. The systems have a combined peak output rating of

approximately 120kW. The CPV system performance was assessed using the data collected from the CPV systems. The CPV system operated with an overall efficiency of 23.63% and a cut in threshold of 350 W/m^2. No correlation between ambient temperature and system efficiency were found. Data collected also revealed that the combined solar generation from the CPV systems and the fixed PV systems coincides with demand during winter months and precedes demand by approximately 1 hour during summer months and serves approximately 4% of peak campus load. Initial analyses done by scaling up the temporal current combined solar generation showed that the maximum allowable combined solar generation (without curtailment or energy storage capabilities) while meeting minimum utility import requirements is approximately 3 MW. Data also revealed excessively high terminal voltages. Possible remedies include increasing the CPV-7700 to ARC-MCC conductor size, operating at a lagging power factor, or utilizing a dedicated step-up transformer to directly couple to the 12kV feeder.

Circuit simulations were performed using two modeling platforms: ETAP and MATLAB. ETAP was used for campus wide traditional load flow studies while MATLAB was used for detailed sub-circuit and investigational simulations. These circuit simulations provided several important conclusions regarding campus circuit operation with installed CPV systems:

- Voltage fluctuations due to changes in power production attributed to cloud cover and coastal fog are adequately buffered by utility voltage up to an installed CPV capacity of 14 MW.
- Net reverse power flow at the ARC-MCC is achieved at approximately 380 kW installed CPV capacity.
- To achieve the highest efficiency, it is recommended that CPV installations occur until the CPV capacity equals the peak electrical demand at that circuit location. Further CPV installations result in increased line losses.
- UC-3, 4, and 10 are ideal candidates for large installations at the 480V level due to their proximity to the UCI substation.
- Installation near the UCI substation results in the greatest voltage stability and minimizes line losses.
- UC-1, 2, 5, 6, 8, and 9 are unable to support any CPV above approximately 360kW at any individual location at the 480V level without exceeding ANSI voltage tolerance limits while operating at unity power factor. Installation at the 12kV feeder may alleviate this issue.